

Characterization of a Unique Pathway for 4-Cresol Catabolism Initiated by Phosphorylation in *Corynebacterium glutamicum*^{*[5]}

Received for publication, October 26, 2015, and in revised form, January 27, 2016. Published, JBC Papers in Press, January 27, 2016, DOI 10.1074/jbc.M115.695320

Lei Du^{‡§}, Li Ma[‡], Feifei Qi[‡], Xianliang Zheng^{‡§}, Chengying Jiang[¶], Ailei Li^{||}, Xiaobo Wan^{||}, Shuang-Jiang Liu^{¶1}, and Shengying Li^{‡2}

From the [‡]CAS Key Laboratory of Biofuels, Shandong Provincial Key Laboratory of Synthetic Biology and the ^{||}CAS Key Laboratory of Bio-based Materials at Qingdao Institute of Bioenergy and Bioprocess Technology, Chinese Academy of Sciences, Qingdao, Shandong 266101, China, the [§]University of the Chinese Academy of Sciences, Beijing 100049, China, and the [¶]State Key Laboratory of Microbial Resources, and Environmental Microbiology and Biotechnology Research Center at Institute of Microbiology, Chinese Academy of Sciences, Beijing 100101, China

4-Cresol is not only a significant synthetic intermediate for production of many aromatic chemicals, but also a priority environmental pollutant because of its toxicity to higher organisms. In our previous studies, a gene cluster implicated to be involved in 4-cresol catabolism, *creCDEFGHIR*, was identified in *Corynebacterium glutamicum* and partially characterized *in vivo*. In this work, we report on the discovery of a novel 4-cresol biodegradation pathway that employs phosphorylated intermediates. This unique pathway initiates with the phosphorylation of the hydroxyl group of 4-cresol, which is catalyzed by a novel 4-methylbenzyl phosphate synthase, CreHI. Next, a unique class I P450 system, CreJEF, specifically recognizes phosphorylated intermediates and successively oxidizes the aromatic methyl group into carboxylic acid functionality via alcohol and aldehyde intermediates. Moreover, CreD (phosphohydrolase), CreC (alcohol dehydrogenase), and CreG (aldehyde dehydrogenase) were also found to be required for efficient oxidative transformations in this pathway. Steady-state kinetic parameters (K_m and k_{cat}) for each catabolic step were determined, and these results suggest that kinetic controls serve a key role in directing the metabolic flux to the most energy effective route.

The aromatic compound 4-cresol (*i.e.* *p*-cresol or *p*-methylphenol) is an important synthetic precursor for manufacturing a great variety of chemical products including synthetic resins, disinfectants, antioxidants, preservatives, fumigants, explosives, and others (1). However, it is also a priority environmental pollutant because of its high toxicity to many higher organisms including humans (2, 3). This compound is mainly derived from diverse industrial processes such as coal gasification and fractionation of coal tar. In nature, 4-cresol is generated by

anaerobic bacteria as a byproduct during the metabolism of phenylalanine and tyrosine (4–6).

Like other aromatic compounds, 4-cresol in polluted environments is degraded by various aerobic and anaerobic microorganisms. Thus, studies on biodegradation mechanisms of 4-cresol hold significant potential for industrial application in environmental protection. In the past decades, a growing number of microorganisms capable of degrading 4-cresol have been discovered, and great efforts have been made to elucidate their biodegradation pathways (7–16).

Currently known 4-cresol catabolic pathways can be classified into one of three categories based on the initial step (Fig. 1). The microorganisms falling into the first category (Fig. 1A) begin their degradation of 4-cresol from a methyl hydroxylation step. For instance, in Gram-negative *Pseudomonas* species, 4-cresol is initially oxidized to 4-hydroxybenzyl alcohol, and then to 4-hydroxybenzyl aldehyde by the same enzyme 4-cresol methylhydroxylase (PCMH)³ (17–20). Subsequently, 4-hydroxybenzyl aldehyde undergoes variant modifications to form protocatechuic acid (*i.e.* 3,4-dihydroxybenzoate) or benzoyl-CoA, both of which can be diverted into the central metabolism (*i.e.* TCA) (9, 13, 15, 19, 21).

In the second category, the obligate anaerobe *Desulfobacterium cetonicum* (12) initiates the degradation of 4-cresol by linking a fumarate moiety to the methyl group to generate 4-hydroxybenzyl succinate, which is further degraded to 4-hydroxybenzoyl-CoA via β -oxidation (Fig. 1B). Subsequent reduction to benzoyl-CoA leads the metabolic flux to the central metabolism.

The fungus *Aspergillus fumigates* likely adopts the third type of degradation pathway to assimilate 4-cresol (14). To form protocatechuic acid, the hydroxylation of 4-cresol by an NADPH-dependent hydroxylase first occurs on aromatic ring to produce 4-methylcatechol, followed by a series of methyl oxidations (Fig. 1C). The intermediates and the enzyme activities for the proposed steps have been identified using cell free extracts (14). In yeast *Trichosporon cutaneum* (16), an ortho-fission enzyme directly transforms 4-methyl-

^{*} This work was supported by National Natural Science Foundation of China under Grant NSFC 31422002 and Shandong Provincial Natural Science Foundation Grant JQ201407, and the funding from Recruitment Program of Global Experts (to S. L.) and 973 Project from Ministry of Science and Technology Grant 2012CB7211-04 (to S.-J. L.). The authors declare that they have no conflicts of interest with the contents of this article.

^[5] This article contains supplemental Tables S1 and S2 and Figs. S1–S25.

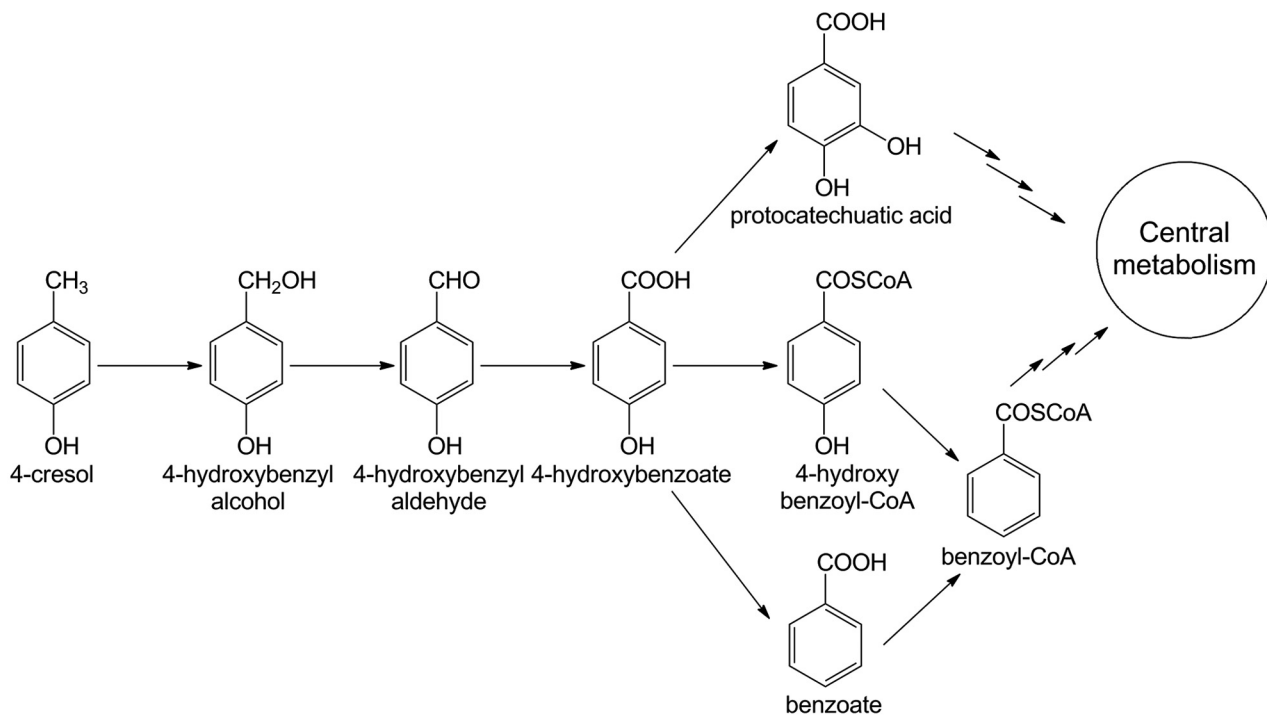
¹ To whom correspondence may be addressed. E-mail: liusj@im.ac.cn.

² To whom correspondence may be addressed. E-mail: lishengying@qibebt.ac.cn.

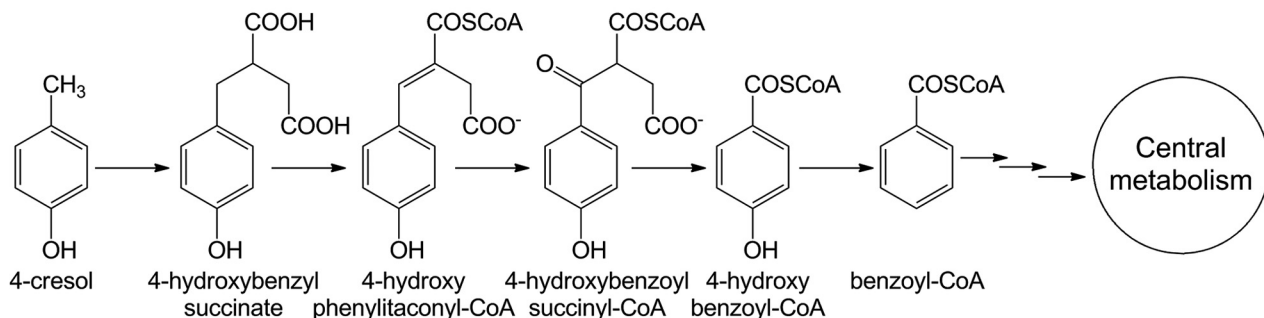
³ The abbreviations used are: PCMH, 4-cresol methylhydroxylase; P450, cytochrome P450 enzyme; HRMS, high resolution mass spectrometry; PEP, phosphoenolpyruvate.

4-Cresol Catabolic Pathway Initiated by Phosphorylation

A



B



C

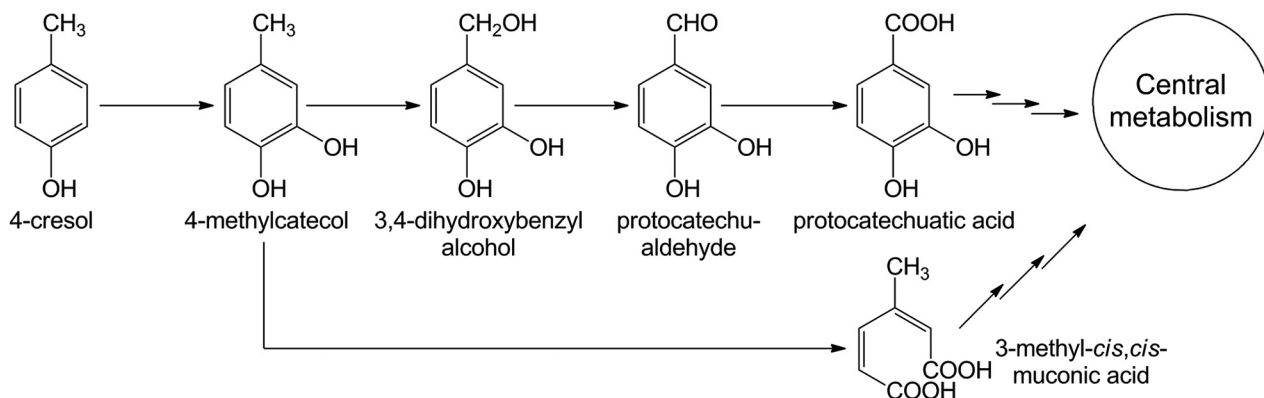


FIGURE 1. **Known pathways for 4-cresol catabolism by variant microorganisms.** Degradation of 4-cresol begins from methyl hydroxylation (A), linking fumarate to the methyl group (B), and direct aromatic ring hydroxylation (C).

catechol into 3-methyl-*cis,cis*-muconic acid, which can readily enter the central metabolism via the β -ketoacid pathway (8) (Fig. 1C).

More recently, focus has shifted toward understanding the capacity of the Gram-positive bacterium *Corynebacterium glutamicum* to metabolize diverse aromatic compounds including

4-cresol (22–31). This high GC content bacterium is not only an important industrial microorganism for production of amino acids and vitamins (32–37), but is also a useful model system to understand the genetics, biochemistry, and mechanisms for biodegradation, especially for assimilation of aromatic compounds (23).

In our previous studies, we employed proteomic analysis and genome mining to identify a gene cluster in *C. glutamicum*, *creABCDEFGHIJR*, which is involved in 4-cresol catabolism (22, 26). Specifically, six (*creD*, *creE*, *creG*, *creH*, *creI*, and *creJ*) of eleven *cre* genes were successfully knocked out from the genome of *C. glutamicum* RES167. Each knock-out strain lost the ability of the wild-type strain to grow in the minimal medium in which 4-cresol was the sole carbon source. For each mutant, genetic complementation with the corresponding gene restored the wild-type phenotype (22). These results clearly demonstrated that at least these six genes were required for 4-cresol biodegradation in *C. glutamicum*. Furthermore, subjecting the six mutants to medium containing diverse aromatic compounds as the sole carbon source, such as 4-hydroxybenzyl alcohol, 4-hydroxybenzyl aldehyde, and 4-hydroxybenzoate, suggested a catabolic pathway responsible for the degradation of 4-cresol (22). However, details of this putative catabolic pathway could not be rationalized from our previous experiments.

Although the *cre* pathway was genetically identified in part, the catalytic functions of the majority of enzymes were not determined. Of the remaining five genes in the pathway, *creR* is a putative regulatory gene and is therefore not predicted to function as a catabolic catalyst. Based on bioinformatics analysis, *creA* and *creB* are believed to reside outside of the *cre* gene cluster boundary. Interestingly, both *Corynebacterium efficiens* YS-314 and *Arthrobacter* sp. FB24 possess the identical *cre* genetic organization to that of *C. glutamicum* with the noted absence of homologues to *creA* and *creB*. Previously, we generated the *creA* and *creB* deletion mutant in *C. glutamicum* and observed that each resulting strain grew similarly to wild type on the medium supplemented with 4-cresol (22). Thus, neither *creA* nor *creB* are predicted to be involved in 4-cresol biodegradation. Finally, numerous attempts to generate *creC* and *creF* deletion mutants were unsuccessful. Therefore, the role of these gene products in 4-cresol degradation could not be anticipated.

In the current work, all biodegradation enzymes encoded by the *cre* gene cluster of *C. glutamicum* were cloned, expressed, and functionally characterized using *in vitro* enzymatic assays. Through these efforts, an unprecedented 4-cresol catabolic pathway was unveiled that features a novel activating mechanism and a group of enzymes possessing remarkable substrate flexibility. Of particular interest, a unique phosphorylation reaction mediated by CreHI was identified as a novel initiating step of 4-cresol biodegradation. Further, a class I cytochrome P450 (P450) system (38) consisting of CreJ (P450 enzyme), CreF (ferredoxin), and CreE (ferredoxin reductase) was elucidated during this investigation. *In vitro* characterization of this system demonstrated that it accepts multiple phosphorylated aromatic compounds as substrates and plays a central role in assimilation of 4-cresol.

Experimental Procedures

Strains, Plasmids, and Culture Conditions—The bacterial strains and plasmids used in this study are listed in supplemental Table S1. *C. glutamicum* was routinely cultivated in Luria-Bertani (LB) broth with a rotary shaker (150 rpm) at 30 °C. *Escherichia coli* strains were grown at 37 °C in LB broth with a rotary

shaker (220 rpm) or on LB agar (2% w/v) plates. For protein expression and purification, *E. coli* strains were cultured in Terrific Broth medium (39). When required, kanamycin was added to a final concentration of 50 µg/ml. *E. coli* DH5α was used for plasmid construction, storage, and isolation. *E. coli* BL21 (DE3) was used for recombinant protein expression.

DNA Isolation and Manipulation—The genomic DNA of *C. glutamicum* was isolated by following the Kirby mix procedure (40). Plasmid DNA was isolated using an E.Z.N.A.™ plasmid miniprep kit (Omega Biotek, Norcross, GA). DNA fragments were purified using the Wizard SV Gel and PCR Clean-up System (Promega, Madison, WI). Ligation, transformation, agarose gel electrophoresis, and other standard techniques for *E. coli* were performed as previously described (41).

Construction of Expression Vectors for *cre* Genes—The complete open reading frames of *creC*, *creD*, *creE*, *creF*, *creG*, *creH*, *creI*, and *creJ* were PCR-amplified (35 cycles of 95 °C for 20s, 62 °C for 20s, and 72 °C for 60s) from genomic DNA of *C. glutamicum* using *Pfu* DNA polymerase (Transgen, Beijing, China). Primers used to amplify the DNA fragments of target genes are listed in supplemental Table S2. Appropriate restriction sites were introduced into the PCR primers for cloning purposes. Resulting PCR amplicons were doubly digested with a specific pair of restriction enzymes and ligated into similarly digested pET-28b (Novagen). All plasmid constructs were confirmed by DNA sequencing (Sangon Biotech, Shanghai, China). Upon sequence verification, plasmids were then transformed into *E. coli* BL21 (DE3) for protein expression.

Protein Expression and Purification—The *E. coli* BL21 (DE3) cells harboring the expression plasmids were grown at 37 °C overnight in LB broth containing 50 µg/ml kanamycin. The overnight culture was used as the seed culture to inoculate (1:100 dilution) 1 liter of Terrific Broth medium containing 5% (w/v) glycerol. The cells were grown at 37 °C with shaking until the A_{600} reached ~0.6. Protein expression was initiated by adding isopropyl β-D-1-thiogalactopyranoside to a final concentration of 0.2 mM. Cultivation continued at 18 °C for an additional 20 h. Purification of His-tagged proteins was carried out as described elsewhere (42) with minor modifications. All protein purification steps were performed at 4 °C. Briefly, the cultures were harvested by centrifugation (5000 × *g* for 5 min). The cell pellet was resuspended in 40 ml of lysis buffer (50 mM NaH₂PO₄, 300 mM NaCl, 10% (w/v) glycerol, and 10 mM imidazole, pH 8.0), and the resuspended cells were lysed by sonication. The cell lysate was clarified by centrifugation at 12,000 × *g* for 30 min to remove cellular debris. Nickel-nitrilotriacetic acid resin (1 ml) (Qiagen) was added to each cell lysate with subsequent incubation with gentle agitation for 30 min. This slurry was loaded into an empty column and washed with ~200 ml of wash buffer (50 mM NaH₂PO₄, 300 mM NaCl, 10% (w/v) glycerol, and 20 mM imidazole, pH 8.0) until no protein was detected in flow-through. Next, the nickel-bound protein was eluted from the resin with 10 ml of elution buffer (50 mM NaH₂PO₄, 300 mM NaCl, 10% (w/v) glycerol, and 250 mM imidazole, pH 8.0). The collected eluent was concentrated with an Amicon Ultra centrifugal filter (Merck) and exchanged into desalting buffer (50 mM NaH₂PO₄, 10% (w/v) glycerol, pH 7.5) using a PD-10 desalting column (GE Healthcare). The resulting

4-Cresol Catabolic Pathway Initiated by Phosphorylation

purified proteins were flash frozen by liquid nitrogen and stored at -80°C for future use.

Purity Qualification and Concentration Determination of Purified Proteins—The purity of all purified proteins was evaluated by SDS-PAGE (supplemental Fig. S1). The concentration of P450 enzyme CreJ was determined according to the method described by Omura and Sato (43). Briefly, the CO-bound reduced difference spectrum of CreJ was recorded by a UV-visible spectrophotometer DU 800 (Beckman Coulter, Fullerton, CA). The concentration of functional P450 was subsequently calculated using the extinction coefficient ($\epsilon_{450-490}$) of $91,000\text{ M}^{-1}\text{cm}^{-1}$. Concentrations of non-P450 enzymes were determined by the Bradford method using BSA as the standard (44).

Enzymatic Assays—The assay employed to evaluate the activity of CreHI was developed based on the previous report by Schmeling *et al.* (45). The reaction mixture contained 1.0 mM of 4-cresol, 4-hydroxybenzyl alcohol, 4-hydroxybenzyl aldehyde, or 4-hydroxybenzoate as substrate, 20 mM MgCl_2 , 1 mM MnCl_2 , 2 mM ATP, and 40 μM purified CreH and CreI.

For the assay of CreD, the reaction mixture contained 1.0 mM of 4-methylbenzyl phosphate, benzylalcohol-4-phosphate, benzylaldehyde-4-phosphate, or benzoate-4-phosphate as substrate; 20 mM MgCl_2 ; and 40 μM purified CreD.

For the assay of P450 monooxygenase activity (CreJEF), the reaction mixture contained 1.0 mM of 4-methylbenzyl phosphate, benzylalcohol-4-phosphate, or benzylaldehyde-4-phosphate as substrate, 2.0 mM NADPH, and 40 μM CreE, CreF, and CreJ (42).

The assays of CreG and CreC were performed following the previous method (22) with minor modifications. In brief, the reaction system was comprised of 1.0 mM alcohol substrate (for CreG) or aldehyde substrate (for CreC), 2.0 mM electron acceptor (NAD^+ for CreG, NADP^+ for CreC), and 40 μM purified CreG or CreC.

For the one-pot reaction, 200 μM 4-cresol was added, and all involved enzymes were normalized to the same concentration of 12 μM . All the above described assays were carried out in 100 mM Tris-HCl buffer (pH 8.0) at 30°C for 120 min. Reactions were quenched by the 1:1 addition of methanol (MeOH) containing 0.2% (v/v) TFA.

Enzymatic Kinetics—The K_m value of each enzyme was determined under the identical condition for its enzymatic activity assay (see above). The concentration of substrates varied from 0.1 to 15 mM, and any required cofactors were added to excess. Each enzyme was diluted to a suitable concentration to ensure that the consumption of substrate was within the linear range during the reaction. Samples from each reaction were taken at 0, 2, and 5 min. The concentrations of products or substrates were determined based on the integrations of chromatographic peak areas observed during HPLC analysis. The K_m and k_{cat} values were calculated by nonlinear regression fitting to the Michaelis-Menten equation. All reactions were carried out in triplicate, and the data were reported as the means \pm S.D.

Analytical Methods—Reaction mixtures in MeOH/ H_2O (1:1) with protein removed by centrifugation ($20,000 \times g$ for 10 min) were analyzed on an Agilent 1260 infinity HPLC system (Ag-

ilent Technologies) equipped with an ultraviolet detector. Specifically, compounds were separated on a ZORBAX SB-C18 column (Agilent Technologies, Wilmington, DE) using a linear mobile phase gradient that ranged from 2% (v/v) MeOH in 0.1% (v/v) TFA aqueous solution to 70% (v/v) MeOH in 0.1% (v/v) TFA aqueous solution over 20 min at a flow rate of 1 ml/min. The wavelength of detection was 275 nm. Structural identification was performed by comparison of retention times of detected compounds with corresponding synthesized authentic standards. Further, eluents were collected and subjected to high resolution mass spectrometry (HRMS) examination. Spectra of electrospray ionization-MS were recorded in the negative ionization mode on an LCQ Deca XP^{plus} ion trap mass spectrometer (Thermo-Finnigan, San Jose, CA).

Chemical Synthesis of Phosphorylated Compounds—The phosphorylated compounds were synthesized through chemical methods with reference to previous reports by McKenna *et al.* (46) and Kenner and Williams (47) (supplemental Fig. S2). The specific procedures are detailed in the supplemental materials. The structures of all the synthetic phosphorylated compounds were confirmed through NMR spectroscopy (supplemental Figs. S3–S8). Benzoate-4-phosphate was produced from benzylaldehyde-4-phosphate through enzymatic reaction catalyzed by the cytochrome P450 system composed of CreJ, CreE, and CreF. The proteins of this enzymatic system in crude benzoate-4-phosphate solution were removed through heat denaturation and centrifugation.

Results

4-Cresol Is Activated via Phosphorylation by a New 4-Methylbenzyl Phosphate Synthase CreHI—Based on our previous genetic knock-out and complementation studies of *cre* genes and also on the identification of the metabolic intermediate 4-hydroxybenzoate (22), it was deduced that the class I P450 system (48) encoded by *creJEF* might be involved in the initial oxidation of 4-cresol. Similar hydroxylation of the methyl group by 4-cresol methylhydroxylase (a flavocytochrome) has been identified in *Pseudomonas putida* (49) and *Geobacter metallireducens* (50). However, we failed to detect hydroxylation of 4-cresol in reactions employing the CreJEF P450 system. Moreover, when we tested the *in vitro* ability of individual enzymes (CreC, CreD, CreG, CreH, or CreI), in the presence of required cofactors, to hydroxylate 4-cresol, no conversion was observed (data not shown). Taken together, these results suggest that an enzyme complex might be required for initiating the modification of 4-cresol.

Subsequent bioinformatics analysis revealed that CreH contains a phosphoenolpyruvate (PEP)-utilizing enzyme mobile domain (supplemental Fig. S9), whereas CreI contains a PEP/pyruvate binding domain (supplemental Fig. S9) (51). Their homologues Orf1 and Orf2 subunits identified in *Thauera aromatica*, which have 62%/45% and 63%/46% amino acid similarity/identity to CreH and CreI, respectively, were reported to be responsible for converting phenol into phenylphosphate when acting synergistically (45). In view of this report, as well as the structural similarity between 4-cresol and phenol, we hypothesized that CreH and CreI might be required in tandem to phosphorylate 4-cresol.

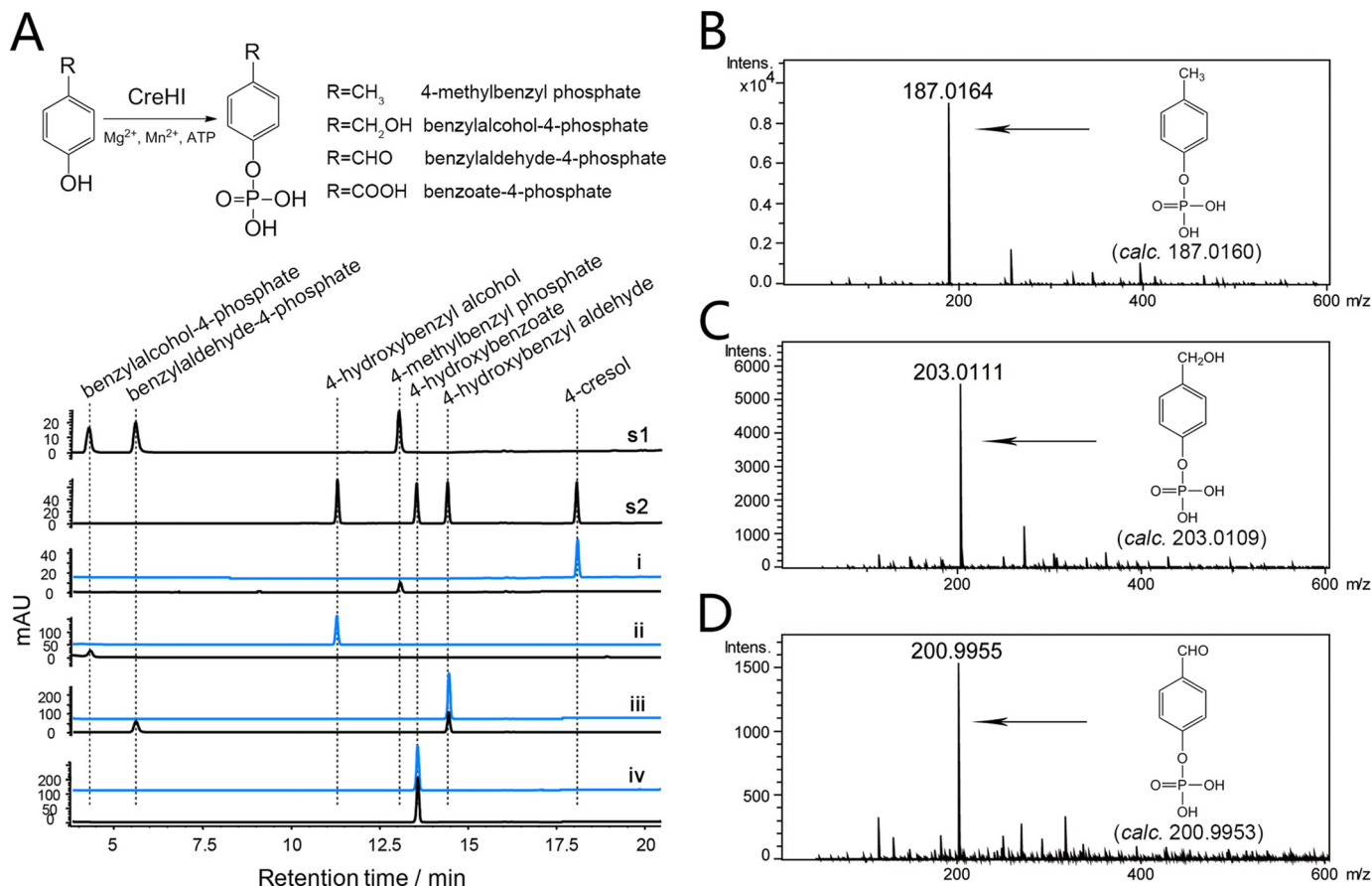


FIGURE 2. **CreHI catalyzed reactions.** *A*, upper panel, CreHI reaction scheme. Lower panel, HPLC analysis (275 nm) of CreHI catalyzed reactions. *s1* and *s2*, authentic standards; *i*, 4-cresol as substrate; *ii*, 4-hydroxybenzyl alcohol as substrate; *iii*, 4-hydroxybenzyl aldehyde as substrate; *iv*, 4-hydroxybenzoate as substrate. Traces in blue represent corresponding control reactions without the addition of enzymes. *B*, HRMS of 4-methylbenzyl phosphate. *C*, HRMS of benzylaldehyde-4-phosphate. *D*, HRMS of benzylaldehyde-4-phosphate. Note that because of distinct extinction coefficients, the peak intensity of compounds do not necessarily reflect relative amounts.

To test this hypothesis, recombinant CreH and CreI were produced and purified from *E. coli* (supplemental Fig. S1), and their combined *in vitro* catalytic activity against 4-cresol was evaluated. In the reaction mixture containing both CreH and CreI, as well as ATP, Mg^{2+} , and Mn^{2+} (all required), 4-cresol was converted to a new product (Fig. 2A). The identity of this product was determined to be 4-methylbenzyl phosphate by HRMS (Fig. 2B) and was confirmed by comparison with the chemically synthesized authentic standard (Fig. 2A). CreHI was also able to catalyze the phosphorylation of 4-hydroxybenzyl alcohol/aldehyde (but not 4-hydroxybenzoate), into their corresponding phosphorylated products benzylalcohol-4-phosphate and benzylaldehyde-4-phosphate, respectively (Fig. 2, A, C, and D). A similar ion-dependent phenylphosphate synthase has been discovered in an anaerobic phenol degrading *T. aromatica* strain (45); however, the newly identified CreHI 4-methylbenzyl phosphate synthase differentiates from the *T. aromatica* phenylphosphate synthase by featuring a distinct substrate profile.

CreJEF Represents a Unique Class I Cytochrome P450 System That Successively Oxidizes 4-Methylbenzyl Phosphate, Benzylalcohol-4-phosphate, and Benzylaldehyde-4-phosphate—Based on DNA sequence analysis, *creJ* putatively encodes a cytochrome P450 enzyme. The coexistence of the ferredoxin gene *creF* and the ferredoxin reductase gene *creE* in the same

gene cluster strongly suggests that CreJEF should form a three-component class I cytochrome P450 system (52). CreJEF cannot directly oxidize 4-cresol; however, the discovery that CreHI produces phosphorylated products naturally led to the hypothesis that CreJEF might require phosphorylated substrate(s). As expected, CreJEF recognized 4-methylbenzyl phosphate as substrate. Interestingly, three products were observed (Fig. 3A), two of which were identified as benzylalcohol-4-phosphate and benzylaldehyde-4-phosphate (see above). The third product was determined to be benzoate-4-phosphate based on HRMS (Fig. 3B) and the proton NMR of the enzymatically prepared product (supplemental Fig. S10). Not surprisingly, CreJEF also catalyzed the oxidation of benzylalcohol-4-phosphate and benzylaldehyde-4-phosphate (Fig. 3A). Taken together, our results demonstrate that CreJEF is a class I P450 system that catalyzes the sequential oxidations from 4-methylbenzyl phosphate to benzoate-4-phosphate.

CreG Is a 4-Hydroxybenzyl Alcohol Dehydrogenase—It was previously reported that *creG* encodes an NAD^+ -dependent 4-hydroxybenzyl alcohol dehydrogenase that oxidizes 4-hydroxybenzyl alcohol into 4-hydroxybenzyl aldehyde (22). In the present work, we further demonstrated that CreG was also able to oxidize benzylalcohol-4-phosphate into benzylaldehyde-4-phosphate (Fig. 4A). Steady-state kinetic analysis indicated that CreG had higher affinity to benzylalcohol-4-phosphate ($K_m =$

4-Cresol Catabolic Pathway Initiated by Phosphorylation

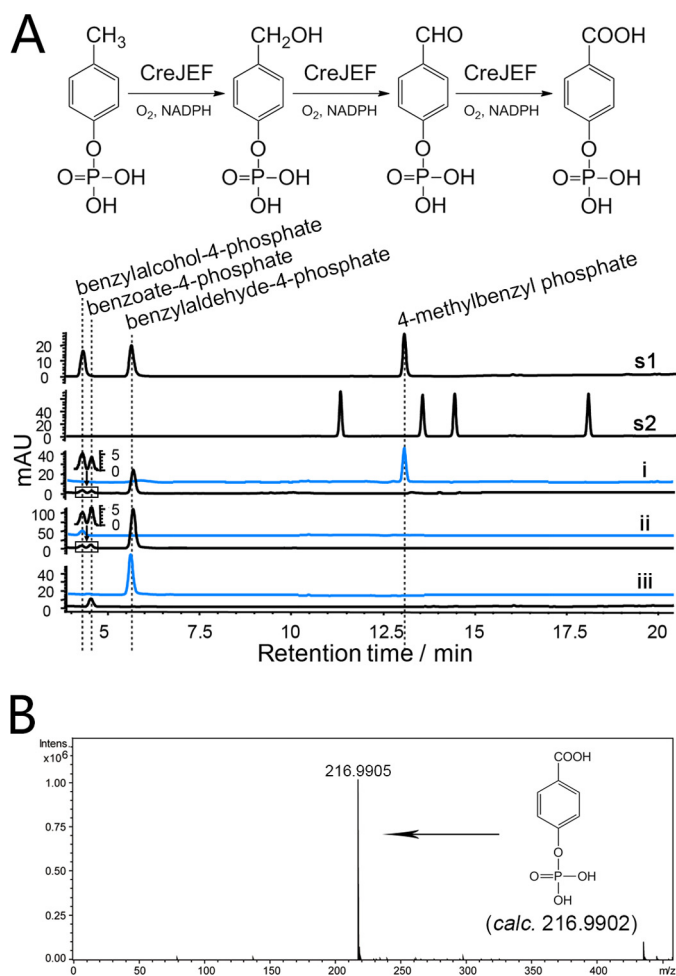


FIGURE 3. CreJEF catalyzed reactions. *A*, upper panel, CreJEF reactions scheme. Lower panel, HPLC analysis (275 nm) of CreJEF catalyzed reactions. *s1* and *s2*, authentic standards; *i*, 4-methylbenzyl phosphate as substrate; *ii*, benzylalcohol-4-phosphate as substrate; *iii*, benzaldehyde-4-phosphate as substrate. Traces in blue represent corresponding control reactions without addition of enzymes. *B*, HRMS of benzoate-4-phosphate. Note that because of distinct extinction coefficients, the peak intensity of compounds do not necessarily reflect relative amounts.

1.2 ± 0.3 mM) than to 4-hydroxybenzyl alcohol ($K_m = 9.4 \pm 0.2$ mM) (Table 1). Notably, CreG used NAD^+ as a preferred cofactor. The dehydrogenase activity of CreG supported by NADP^+ was observed to be 1.3×10^3 times lower than that by NAD^+ , when 4-hydroxybenzyl alcohol was employed as substrate.

CreC Is a Benzaldehyde-4-phosphate Dehydrogenase—Conserved domain searches suggested that CreC belongs to the aldehyde dehydrogenase superfamily containing an aldehyde dehydrogenase domain and an NAD(P)^+ cofactor-binding domain. Based on protein sequence alignment, CreC displays 34% amino acid identity to PcuC, a known 4-hydroxybenzyl aldehyde dehydrogenase from *Pseudomonas* species (7, 8). Catalytically, CreC was able to oxidize both 4-hydroxybenzyl aldehyde and benzaldehyde-4-phosphate to corresponding carboxylic acids (Fig. 4B), respectively. Evaluation of the catalytic efficiency with both substrates revealed that CreC was much more efficient in its ability to oxidize benzaldehyde-4-phosphate ($k_{\text{cat}}/K_m = 1.2 \times 10^4 \text{ mM}^{-1} \text{ min}^{-1}$) than in oxidizing 4-hydroxybenzyl aldehyde ($k_{\text{cat}}/K_m = 77 \text{ mM}^{-1} \text{ min}^{-1}$) (Table 1). Unlike CreG, CreC can only employ NADP^+ as a cofactor,

because no catalytic activity was detected in the presence of NAD^+ . This feature is distinct to other benzylaldehyde dehydrogenases, which have been reported to have the capacity to utilize both NAD^+ and NADP^+ as cofactors (53–55).

CreD Is a Universal Phosphohydrolase—Our previous study demonstrated that CreD displayed phosphohydrolase activity against the unnatural substrate 4-nitrophenylphosphate (22). However, its physiological function remained elusive because there were no substrate candidates available for testing at that time. In this work, the discovery that CreHI catalysis produced phosphorylated products inspired us to examine the activity of CreD against these phosphorylated compounds. As expected, CreD hydrolyzed 4-methylbenzyl phosphate, benzylalcohol-4-phosphate, benzaldehyde-4-phosphate, and benzoate-4-phosphate into 4-cresol, 4-hydroxybenzyl alcohol, 4-hydroxybenzyl aldehyde, and 4-hydroxybenzoate, respectively (Fig. 5).

In Vitro Assembly of the 4-Cresol Catabolic Pathway—Elucidation of the catalytic activities of CreHI, CreJEF, CreG, CreC, and CreD has led to the proposal of a unique 4-cresol biodegradation pathway in *C. glutamicum* (Fig. 6). This pathway has two unusual features. First, all involved biocatalysts can accept multiple metabolic intermediates as substrates, which results in two alternative but interactive routes. The first route of 4-cresol degradation proceeds through phosphorylated intermediates (steps 1 \rightarrow 3 \rightarrow 4 \rightarrow 10 \rightarrow 14), whereas the second route proceeds through nonphosphorylated compounds (steps 1 \rightarrow 3 \rightarrow 7 \rightarrow 8 \rightarrow 13). Second, CreHI and CreD catalyze reverse reactions. This unique paradigm appears to be energy wasteful because the net outcome of ATP consuming phosphorylation reaction catalyzed by CreHI plus phosphohydrolysis by CreD is equivalent to the uneconomical consumption of ATP.

To understand this seemingly unreasonable network with enzyme functional redundancies (*i.e.* a common reaction catalyzed by different enzymes) and unfavorable energy economy, we carried out a one-pot enzymatic reaction to evaluate the efficiency of ATP utilization. In this one-pot pathway reconstitution experiment, all enzymes were normalized to the same concentrations ($12.0 \mu\text{M}$) in the reaction mixture containing $200 \mu\text{M}$ of 4-cresol and all required cofactors. This experimental design is based on the assumption that all involved enzymes are physiologically expressed simultaneously. This assumption was supported by a series of RT-PCR experiments. To determine whether all *cre* genes were expressed coordinately, we attempted to amplify all intergenic regions between two adjacent genes within the *cre* cluster using a common cDNA sample as template. The RT-PCR results (supplemental Fig. S11) indicate that *creC-R* were transcribed as a single operon and likely expressed coordinately. However, the cellular enzyme levels could vary dynamically because of differential affinity of ribosome binding sites across the polycistronic mRNA or diverse epigenetic effects. Thus, the one-pot reaction containing the same levels of enzymes represented a simplified model system for understanding the kinetic behavior of mixed 4-cresol degrading enzymes.

To initiate the multienzymatic catalysis, varying ATP doses ($200, 400,$ and $600 \mu\text{M}$, corresponding to molar ratios of 1:1, 1:2, and 1:3 for -cresol:ATP, respectively) were added into the reaction mixtures. Results showed that 40.8% and 78.8% of 4-cresol

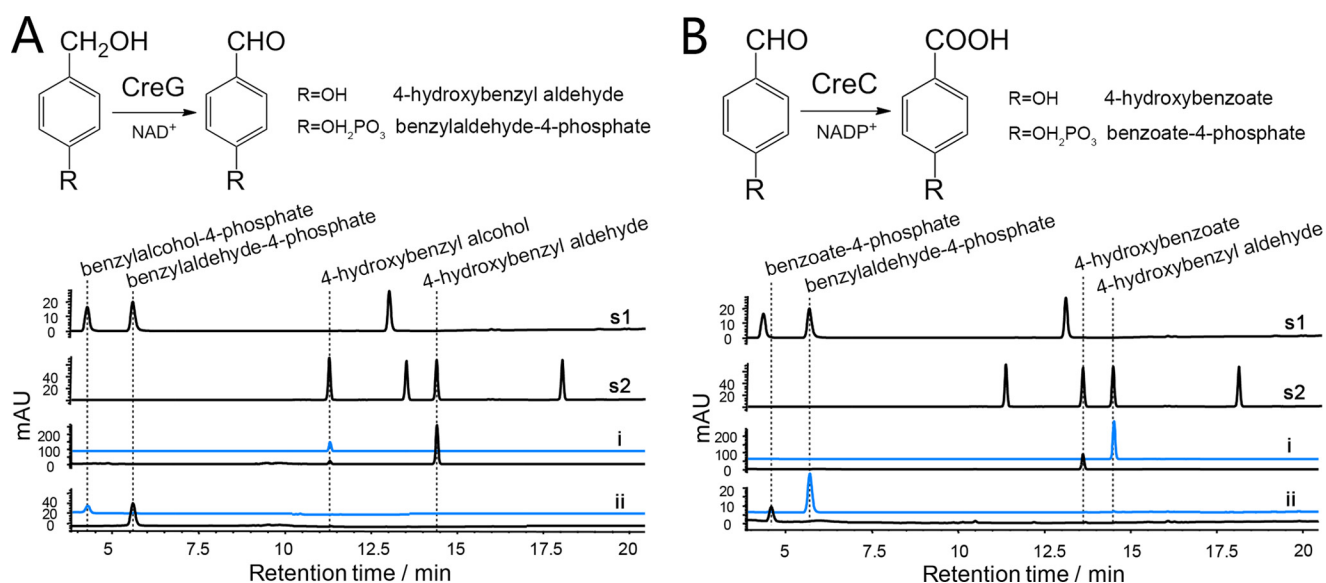


FIGURE 4. **Reactions catalyzed by CreG and CreC.** *A, upper panel*, CreG reactions scheme. *Lower panel*, HPLC analysis (275 nm) of CreG catalyzed reactions. *s1* and *s2*, authentic standards; *i*, 4-hydroxybenzyl alcohol as substrate; *ii*, benzylalcohol-4-phosphate as substrate. *B, upper panel*, CreC reactions scheme. *Lower panel*, HPLC analysis of CreC catalyzed reactions. *s1* and *s2*, authentic standards; *i*, 4-hydroxybenzyl alcohol as substrate; *ii*, benzylaldehyde-4-phosphate as substrate. Traces in blue represent corresponding control reactions without addition of enzymes. Note that because of distinct extinction coefficients, the peak intensity of compounds do not necessarily reflect relative amounts.

TABLE 1
Steady-state kinetics of enzymes encoded by the *cre* cluster

The values were calculated by nonlinear regression fitting to the Michaelis-Menten equation. All reactions were carried out in triplicate, and the data are reported as means \pm S.D.

Enzyme	Substrate	K_m	k_{cat}	k_{cat}/K_m
		mm	min ⁻¹	mm ⁻¹ min ⁻¹
CreHI	4-Cresol	0.61 \pm 0.06	60.4 \pm 1.8	99
CreHI	4-Hydroxybenzyl alcohol	0.10 \pm 0.03	36.3 \pm 2.7	3.7 $\times 10^2$
CreHI	4-Hydroxybenzyl aldehyde	0.21 \pm 0.02	14.9 \pm 2.7	71
CreJEF	4-Methylbenzyl phosphate	0.34 \pm 0.06	44.5 \pm 2.3	1.3 $\times 10^2$
CreJEF	Benzylalcohol-4-phosphate	0.38 \pm 0.09	5.21 \pm 0.33	14
CreJEF	Benzylaldehyde-4-phosphate	0.90 \pm 0.22	6.61 \pm 0.59	7.4
CreD	4-Methylbenzyl phosphate	0.62 \pm 0.09	40.2 \pm 1.9	65
CreD	Benzylalcohol-4-phosphate	0.52 \pm 0.06	11.3 \pm 1.5	22
CreD	Benzylaldehyde-4-phosphate	0.32 \pm 0.02	23.3 \pm 0.7	72
CreC	4-Hydroxybenzyl aldehyde	0.058 \pm 0.006	4.43 \pm 0.20	77
CreC	Benzylaldehyde-4-phosphate	0.12 \pm 0.04	(1.41 \pm 0.10) $\times 10^3$	1.2 $\times 10^4$
CreG	4-Hydroxybenzyl alcohol	9.4 \pm 0.2	24.8 \pm 0.4	2.6
CreG	Benzylalcohol-4-phosphate	1.2 \pm 0.3	1.74 \pm 0.20	1.5

were consumed when the substrate:ATP ratios were 1:1 and 1:2, respectively. 4-Cresol was completely consumed when the 4-cresol:ATP ratio was 1:3 (Fig. 7A). These quantitative results indicate that 4-cresol can be efficiently converted into downstream metabolic intermediates; meanwhile the futile ATP consumption indeed occurred to some extent.

Enzyme Kinetics Regulates the Metabolic Flux in the 4-Cresol Biodegradation Pathway—To further understand the metabolic flux in the complex 4-cresol catabolic pathway, the steady-state enzymatic kinetic parameters of each step were determined (Table 1 and supplemental Figs. S12–S24). The phosphorylation of 4-cresol by CreHI had an apparent K_m value of 0.61 \pm 0.06 mM and a k_{cat} value of 60.4 \pm 1.8 min⁻¹, resulting in a calculated catalytic efficiency (k_{cat}/K_m) of 99 mm⁻¹min⁻¹ for this initial step. The catalytic efficiency of CreHI was slightly higher than the phosphohydrolysis of 4-methylbenzyl phosphate ($k_{cat}/K_m = 65$ mm⁻¹min⁻¹) by CreD. Interestingly, the oxidation of 4-methylbenzyl phosphate by CreJEF was more efficient than the phosphohydrolysis by

CreD, because CreJEF had lower K_m and higher k_{cat} (\sim 2-fold more efficient than CreD for 4-methylbenzyl phosphate). The competition experiment between CreJEF and CreD showed that the final ratio between oxidation and hydrolysis products was 59:41 (supplemental Fig. S25), which is consistent with the kinetic data.

Next, additional one-pot reactions were performed to evaluate the contribution of CreC and CreG in this catabolic pathway (Fig. 7B). Again, 4-cresol was completely converted to 4-hydroxybenzoate in the one-pot reaction containing all enzymes. When both CreC and CreG were absent, the main products turned out to be 4-hydroxybenzyl alcohol (64.2%) and 4-hydroxybenzyl aldehyde (33.5%), whereas the terminal-product 4-hydroxybenzoate only accounted for 2.3% of all products. This result is consistent with the enzyme kinetic studies, where the k_{cat}/K_m values of step 4 (14 mm⁻¹min⁻¹) and step 9 (7.4 mm⁻¹min⁻¹) were lower than those of step 7 (22 mm⁻¹min⁻¹) and step 12 (72 mm⁻¹min⁻¹), respectively. When only CreC was omitted, 4-hydroxybenzyl aldehyde was the predominant

4-Cresol Catabolic Pathway Initiated by Phosphorylation

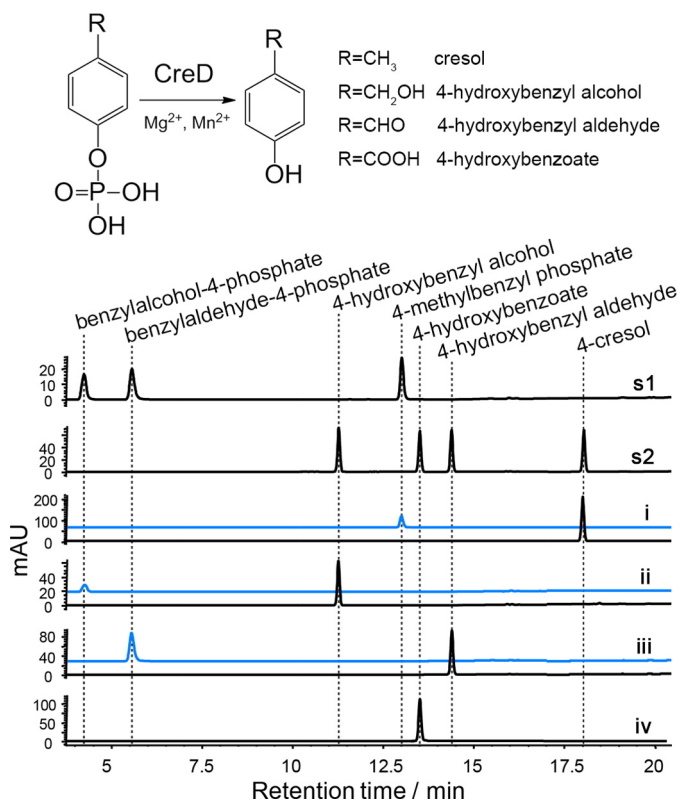


FIGURE 5. **Reactions catalyzed by CreD.** Upper panel, CreD reactions scheme. Lower panel, HPLC analysis (275 nm) of CreD catalyzed reactions. *s1* and *s2*, authentic standards; *i*, 4-methylbenzyl phosphate as substrate; *ii*, benzylalcohol-4-phosphate as substrate; *iii*, benzylaldehyde-4-phosphate as substrate; *iv*, benzoate-4-phosphate as substrate. Traces in blue represent corresponding control reactions without addition of enzymes. Note that because of distinct extinction coefficients, the peak intensity of compounds do not necessarily reflect relative amounts.

product (92.4%), 4-hydroxybenzoate was the minor product (7.6%), whereas 4-hydroxybenzyl alcohol was not detected. If only CreG was omitted, 4-hydroxybenzyl alcohol and 4-hydroxybenzoate accounted for 61.0 and 39.0% of products, respectively. In sum, the involvement of CreC and CreG in the reaction pathway serves to make these oxidative conversions more efficient and energy-effective.

Discussion

Two unusual enzymatic systems represent the most important discoveries of the current study: 1) CreHI initiates the pathway by phosphorylating 4-cresol to give 4-methylbenzyl phosphate, and 2) CreJEF catalyzes the three-step sequential oxidation of 4-methylbenzyl phosphate to benzylalcohol-4-phosphate, benzylaldehyde-4-phosphate, and benzoate-4-phosphate.

Conserved domain searches revealed that CreH has a PEP-utilizing enzyme mobile domain, whereas CreI has a PEP/pyruvate binding domain (51). Interestingly, both CreH and CreI possess respective conserved domains with strong similarity to different parts of the PEP synthase of *E. coli* (supplemental Fig. S9), suggesting a possible evolutionary relationship between CreH, CreI, and PEP synthase. The Orf1 and Orf2 subunits from the anaerobic *T. aromatica*, which show 45 and 46% amino acid identity to CreH and CreI, respectively, are responsible for converting phenol into phenylphosphate (45, 56, 57). The *creHI* homologous genes are also found in many other microbial genomes such as *C. efficiens*, *Cladosporium halotolerans*, *Brevibacterium flavum*, *Arthrobacter* species, *Kocuria palustris*, *Bradyrhizobium* species, and *Runella slithyformis*. Taken together, these gene products may form a new enzyme family capable of phosphorylating phenolic

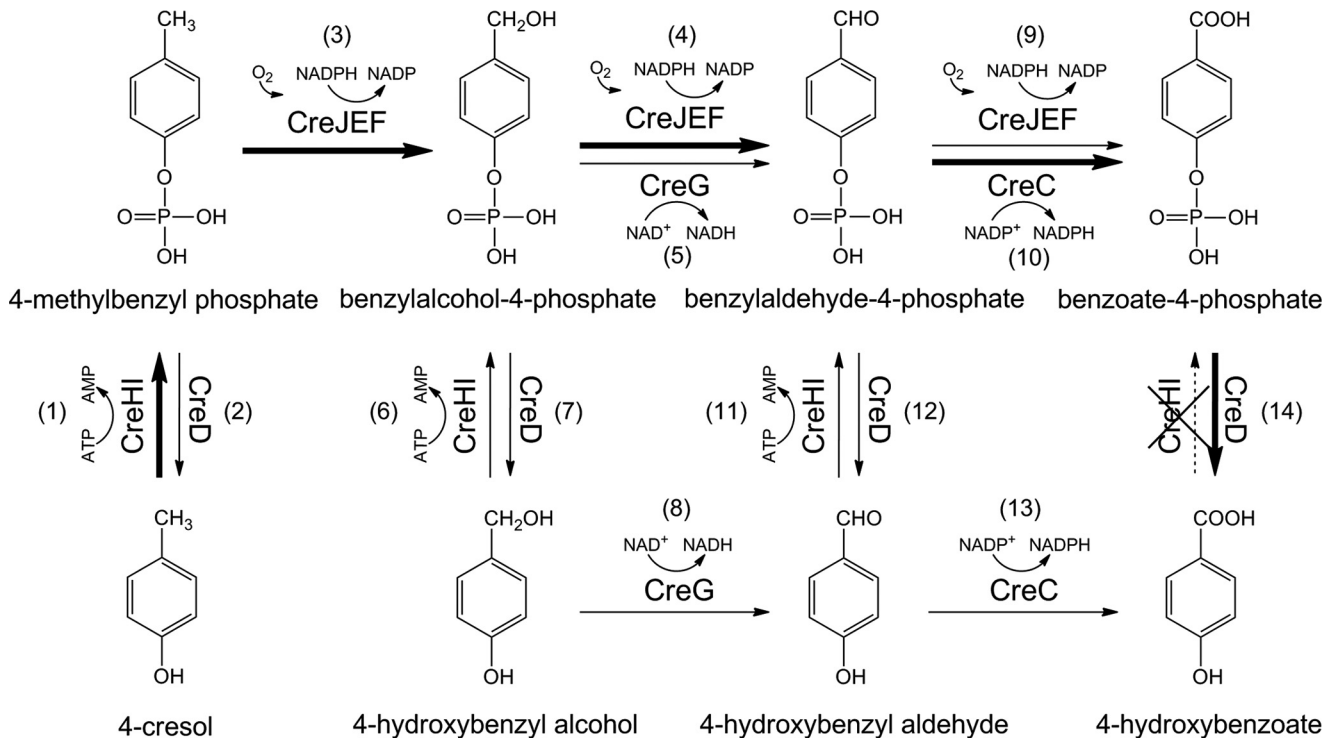


FIGURE 6. **The catabolic pathway for 4-cresol from *C. glutamicum*.** Bold arrows indicate the major phosphorylated pathway comprised of enzymatic steps with greater k_{cat}/K_m values. Each number in bracket denotes an individual enzymatic step.

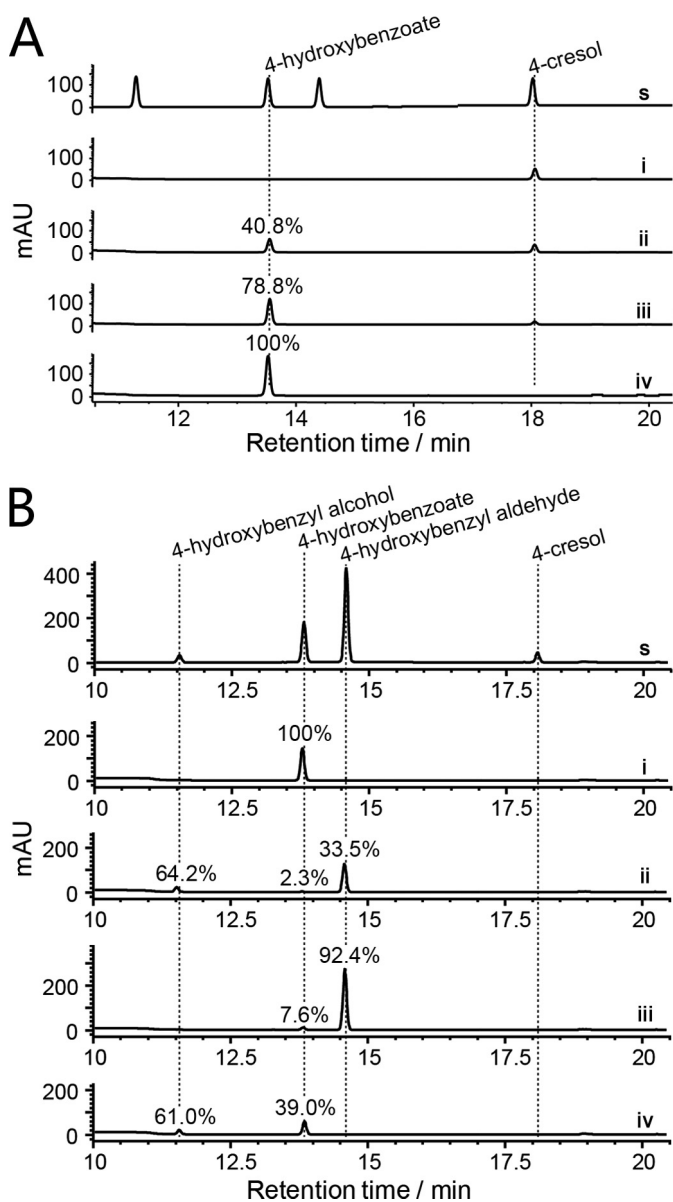


FIGURE 7. One-pot reaction analyses. A, HPLC analysis (275 nm) of the one-pot reaction containing all enzymes (CreHI, CreJEF, CreD, CreG, and CreC) under different molar ratios of 4-cresol:ATP. *s*, authentic standards; *i–iv*, ATP:4-cresol = 0, 1, 2, 3. B, HPLC analysis (275 nm) of the one-pot reaction with different enzyme combinations. *s*, authentic standards; *i*, all enzymes (CreHI, CreJEF, CreD, CreG, and CreC) in one pot; *ii*, all enzymes except CreC and CreG; *iii*, all enzymes except CreC; *iv*, all enzymes except CreG. All involved enzymes were normalized to the same concentration of 12.0 μM . All assays used 200 μM 4-cresol as substrate and were carried out in 100 mM Tris-HCl buffer (pH 8.0) at 30 °C for 120 min. In assays of B, the initial concentration of ATP was 600 μM , and all conversions of 4-cresol were complete. Note that each percentage indicates the conversion ratio from 4-cresol to the specific product. Because of distinct extinction coefficients, the peak intensity of compounds do not necessarily reflect relative amounts shown in percentage.

compounds. Moreover, the genomes of *C. efficiens*, *C. halotolerans*, *B. flavum*, *Arthrobacter* species, and *K. palustris* contain gene clusters with strong homology to the *cre* gene cluster of *C. glutamicum*, suggesting that these bacteria are likely able to degrade 4-cresol using the same mechanism employed by *C. glutamicum*.

CreJEF is able to catalyze the successive oxidations of phosphorylated intermediates. It is possible that the phosphate

group of substrates could act as an anchoring group that delivers the substrate to the correct position within the active site of CreJ, as done by the deoxysugar that is attached to substrates of the PikC P450 enzyme (58, 59). To the best of our knowledge, this is the first reported example of a P450 enzyme that recognizes a spectrum of substrates via a phosphate group. This discovery may have great biotechnological potential for selective oxidation of unactivated C–H bonds.

Some known P450 enzymes are capable of catalyzing the complete oxidation of a C–H bond into a carboxylic group. One important example is the multifunctional *ent*-kaurene oxidase encoded by the P450–4 gene in the gibberellin biosynthetic pathway of *Gibberella fujikuroi*. This P450 enzyme catalyzes three successive oxidation steps between *ent*-kaurene and *ent*-kaurenoic acid (60). Another example is CYP71AV1 from *Artemisia annua*, which performs a three-step oxidation of amorpho-4,11-diene to form artemisinic acid (61). To complete this challenging six-electron oxidation, CYP71AV1 recruits an artemisinic aldehyde dehydrogenase and an alcohol dehydrogenase to achieve the optimal transformation (62). This is similar to what we have observed with CreJEF, CreC, and CreG. Likewise, in the tirandamycin biosynthetic pathway, TamI P450 enzyme employs the FAD-containing TamL oxidase to overcome the conversion from an alcohol to a keto group (63). These examples suggest that the successive oxidations are likely a heavy burden for P450 enzymes to accomplish on their own; therefore, assistance is required from other types of oxidases.

It is obvious that the initial oxidation of 4-cresol requiring a prephosphorylation step in *C. glutamicum* is more complicated than the direct oxidation catalyzed by a 4-cresol methylhydroxylase (PCMH). Kinetically, the latter flavocytochrome is much more efficient. For example, the PCMH from a denitrifying *Achromobacter* sp. exhibited K_m and k_{cat} values for 4-cresol of 21 μM and 112 s^{-1} , respectively (15). The k_{cat}/K_m value of another PCMH from *P. putida* NCIMB 9869 was calculated to be $2.9 \times 10^5 \text{ mM}^{-1} \text{ min}^{-1}$ (17). Both enzymes are >2000 times more efficient than CreJEF using 4-methylbenzyl phosphate as substrate ($K_m = 0.34 \text{ mM}$, $k_{cat} = 44.5 \text{ min}^{-1}$; Table 1). This is not surprising because the k_{cat} values of many P450 enzymes are within 1–300 min^{-1} , which can mainly be attributed to the slow electron transfer step (64). Considering that the additional enzymes in the pathway (except for CreC against benzylaldehyde-4-phosphate) also displayed relatively high K_m and low k_{cat} values (Table 1), *C. glutamicum* appears not to be a good 4-cresol assimilating microorganism. However, without a PCMH gene on its genome (data not shown), it is intriguing to speculate that *C. glutamicum* was forced to evolve a novel, albeit less efficient, pathway for 4-cresol degradation.

Based on the kinetic analyses and competition experiments, we propose that the primary degradation pathway for 4-cresol in *C. glutamicum* is the phosphorylated route (Fig. 6): 4-cresol is first activated by CreHI via conversion into 4-methylbenzyl phosphate, and subsequent oxidations of phosphorylated intermediates are co-mediated by CreJEF, CreG, and CreC. This proposed pathway sequence is supported by the fact that the conversion from benzoate-4-phosphate to 4-hydroxybenzoate is a unidirectional reaction (Fig. 6), because CreHI does not take 4-hydroxybenzoate as substrate.

4-Cresol Catabolic Pathway Initiated by Phosphorylation

However, it remains yet premature to suggest that the primary route consisting of steps 1 → 3 → 4 → 10 → 14 represents the physiological pathway for 4-cresol degradation in *C. glutamicum* because of details lacking with respect to the cellular concentration and localization of enzymes, availability of cofactors, and other intracellular environmental factors. It is noteworthy that there is both agreement as well as inconsistency between the proposed pathway in this study and the previous *in vivo* results (22). For example, according to the pathways shown in Fig. 6, the inactivation of CreJEF, CreHI, or CreD would block the major catabolic pathway, thus abolishing the ability of knock-out strains to grow on 4-cresol as the sole carbon source. This observation is consistent with the previous observations (22). In contrast, based on the results obtained from the one-pot reactions (Fig. 7B), CreG and CreC appear to be unnecessary in the major route from 4-cresol to 4-hydroxybenzoate. This observation, however, contradicts our earlier finding that the *creG* knock-out strain was unable to grow using 4-cresol as the sole carbon source. We reason that this inconsistency might be derived from a yet unknown function of CreG or the result of the complexity within the *in vivo* environment such as balances of energy and cofactors or potential toxicity of produced intermediates that could adversely affect cell growth.

Another interesting aspect of the 4-cresol catabolic pathway is the differential usage of cofactors by CreJEF (NADPH), CreG (NAD⁺), and CreC (NADP⁺). This may be of physiological importance, because these enzymes may rely on a cofactor balancing system during degradation of 4-cresol. For instance, CreJEF and CreC may form an NADPH/NADP⁺ recycling system *in vivo* to avoid too much loss of reducing power during multiple P450 oxidations.

It is intriguing to speculate that the substrate flexibility of the catabolic enzymes involved in 4-cresol degradation may have physiological significance because this pathway could also assimilate other phenolic compounds. To further assess this possibility, we are currently pursuing more detailed biochemical studies in our laboratories. Enzyme function redundancy may be useful when microorganisms face harsh polluted environments because multiple enzymes with a common functionality could maximally release the metabolic potential by better taking advantage of substrates, cofactors, and energy stored in different forms.

Author Contributions—L. D., X. W., S.-J. L., and S. L. conceived this study, analyzed the results, and wrote the manuscript. L. D., L. M., F. Q., X. Z., C. J., and A. L. conducted experiments. All authors read and approved the manuscript.

Acknowledgments—We thank Dr. Shaohua Huang, Dr. Ying Yang, and Fali Bai (Qingdao Institute of Bioenergy and Bioprocess Technology, Chinese Academy of Sciences) for assistance during NMR and LC-MS data collections. We are grateful to Dr. Jeffrey D. Kittendorf (Alluvium Biosciences Inc.) for proofreading the manuscript.

References

1. Fiege, H. (2000) Cresols and Xylenols. in *Ullmann's Encyclopedia of Industrial Chemistry*, John Wiley & Sons, Inc., New York
2. (2008) *Toxicological Profile for Cresols*, Agency for Toxic Substances and Disease Registry, U.S. Department of Health and Human Services, Public Health Service, Atlanta, GA
3. Back, K. C., Thomas, A. A., and MacEwen, J. D. (1972) *Reclassification of Materials Listed as Transportation Health Hazards*, 6570th Aerospace Medical Research Laboratory, Wright-Patterson Air Force Base, Fairborn, OH
4. Curtius, H. C., Mettler, M., and Ettlinger, L. (1976) Study of the intestinal tyrosine metabolism using stable isotopes and gas chromatography-mass spectrometry. *J. Chromatogr.* **126**, 569–580
5. Yu, L., Blaser, M., Andrei, P. I., Pierik, A. J., and Selmer, T. (2006) 4-hydroxyphenylacetate decarboxylases: properties of a novel subclass of glycol radical enzyme systems. *Biochemistry* **45**, 9584–9592
6. Yokoyama, M. T., and Carlson, J. R. (1981) Production of skatole and *para*-cresol by a rumen *Lactobacillus* sp. *Appl. Environ. Microbiol.* **41**, 71–76
7. Cho, A. R., Lim, E. J., Veeranagouda, Y., and Lee, K. (2011) Identification of a *p*-cresol degradation pathway by a GFP-based transposon in *Pseudomonas* and its dominant expression in colonies. *J. Microbiol. Biotechnol.* **21**, 1179–1183
8. Jöesaar, M., Heinaru, E., Viggor, S., Vedler, E., and Heinaru, A. (2010) Diversity of the transcriptional regulation of the *pch* gene cluster in two indigenous *p*-cresol-degradative strains of *Pseudomonas fluorescens*. *FEMS Microbiol. Ecol.* **72**, 464–475
9. Peters, F., Heintz, D., Johannes, J., van Dorsselaer, A., and Boll, M. (2007) Genes, enzymes, and regulation of *para*-cresol metabolism in *Geobacter metallireducens*. *J. Bacteriol.* **189**, 4729–4738
10. Butler, J. E., He, Q., Nevin, K. P., He, Z., Zhou, J., and Lovley, D. R. (2007) Genomic and microarray analysis of aromatics degradation in *Geobacter metallireducens* and comparison to a *Geobacter* isolate from a contaminated field site. *BMC Genomics* **8**, 180
11. Tallur, P. N., Megadi, V. B., Kamanavalli, C. M., and Ninnekar, H. Z. (2006) Biodegradation of *p*-cresol by *Bacillus* sp strain PHN 1. *Curr. Microbiol.* **53**, 529–533
12. Müller, J. A., Galushko, A. S., Kappler, A., and Schink, B. (2001) Initiation of anaerobic degradation of *p*-cresol by formation of 4-hydroxybenzylsuccinate in *Desulfobacterium cetonicum*. *J. Bacteriol.* **183**, 752–757
13. Londry, K. L., Suflita, J. M., and Tanner, R. S. (1999) Cresol metabolism by the sulfate-reducing bacterium *Desulfotomaculum* sp. strain Groll. *Can. J. Microbiol.* **45**, 458–463
14. Jones, K. H., Trudgill, P. W., and Hopper, D. J. (1993) Metabolism of *p*-cresol by the fungus *Aspergillus fumigatus*. *Appl. Environ. Microbiol.* **59**, 1125–1130
15. Hopper, D. J., Bossert, I. D., and Rhodes-Roberts, M. E. (1991) *p*-Cresol methylhydroxylase from a denitrifying bacterium involved in anaerobic degradation of *p*-cresol. *J. Bacteriol.* **173**, 1298–1301
16. Powlowski, J. B., and Dagley, S. (1985) β -Ketoacid pathway in *Trichosporon cutaneum* modified for methyl-substituted metabolites. *J. Bacteriol.* **163**, 1126–1135
17. Efimov, I., Cronin, C. N., Bergmann, D. J., Kuusk, V., and McIntire, W. S. (2004) Insight into covalent flavinylation and catalysis from redox, spectral, and kinetic analyses of the R474K mutant of the flavoprotein subunit of *p*-cresol methylhydroxylase. *Biochemistry* **43**, 6138–6148
18. Cunane, L. M., Chen, Z. W., Shamala, N., Mathews, F. S., Cronin, C. N., and McIntire, W. S. (2000) Structures of the flavocytochrome *p*-cresol methylhydroxylase and its enzyme-substrate complex: gated substrate entry and proton relays support the proposed catalytic mechanism. *J. Mol. Biol.* **295**, 357–374
19. Kim, J., Fuller, J. H., Cecchini, G., and McIntire, W. S. (1994) Cloning, sequencing, and expression of the structural genes for the cytochrome and flavoprotein subunits of *p*-cresol methylhydroxylase from two strains of *Pseudomonas putida*. *J. Bacteriol.* **176**, 6349–6361
20. Mathews, F. S., Chen, Z. W., Bellamy, H. D., and McIntire, W. S. (1991) 3-Dimensional structure of *para*-cresol methylhydroxylase (flavocytochrome-C) from *Pseudomonas putida* at 3.0-Å resolution. *Biochemistry* **30**, 238–247
21. Tallur, P. N., Megadi, V. B., and Ninnekar, H. Z. (2009) Biodegradation of *p*-cresol by immobilized cells of *Bacillus* sp. strain PHN 1. *Biodegradation*

- 20, 79–83
22. Li, T., Chen, X., Chaudhry, M. T., Zhang, B., Jiang, C. Y., and Liu, S. J. (2014) Genetic characterization of 4-cresol catabolism in *Corynebacterium glutamicum*. *J. Biotechnol.* **192**, 355–365
 23. Shen, X. H., Zhou, N. Y., and Liu, S. J. (2012) Degradation and assimilation of aromatic compounds by *Corynebacterium glutamicum*: another potential for applications for this bacterium? *Appl. Microbiol. Biotechnol.* **95**, 77–89
 24. Zhao, K. X., Huang, Y., Chen, X., Wang, N. X., and Liu, S. J. (2010) PcaO positively regulates pcaHG of the β -ketoacid pathway in *Corynebacterium glutamicum*. *J. Bacteriol.* **192**, 1565–1572
 25. Huang, Y., Zhao, K. X., Shen, X. H., Jiang, C. Y., and Liu, S. J. (2008) Genetic and biochemical characterization of a 4-hydroxybenzoate hydroxylase from *Corynebacterium glutamicum*. *Appl. Microbiol. Biotechnol.* **78**, 75–83
 26. Qi, S. W., Chaudhry, M. T., Zhang, Y., Meng, B., Huang, Y., Zhao, K. X., Poetsch, A., Jiang, C. Y., Liu, S., and Liu, S. J. (2007) Comparative proteomes of *Corynebacterium glutamicum* grown on aromatic compounds revealed novel proteins involved in aromatic degradation and a clear link between aromatic catabolism and gluconeogenesis via fructose-1,6-bisphosphatase. *Proteomics* **7**, 3775–3787
 27. Chaudhry, M. T., Huang, Y., Shen, X. H., Poetsch, A., Jiang, C. Y., and Liu, S. J. (2007) Genome-wide investigation of aromatic acid transporters in *Corynebacterium glutamicum*. *Microbiology* **153**, 857–865
 28. Huang, Y., Zhao, K. X., Shen, X. H., Chaudhry, M. T., Jiang, C. Y., and Liu, S. J. (2006) Genetic characterization of the resorcinol catabolic pathway in *Corynebacterium glutamicum*. *Appl. Environ. Microbiol.* **72**, 7238–7245
 29. Brinkrolf, K., Brune, I., and Tauch, A. (2006) Transcriptional regulation of catabolic pathways for aromatic compounds in *Corynebacterium glutamicum*. *Genet. Mol. Res.* **5**, 773–789
 30. Shen, X. H., Jiang, C. Y., Huang, Y., Liu, Z. P., and Liu, S. J. (2005) Functional identification of novel genes involved in the glutathione-independent gentisate pathway in *Corynebacterium glutamicum*. *Appl. Environ. Microbiol.* **71**, 3442–3452
 31. Shen, X. H., Huang, Y., and Liu, S. J. (2005) Genomic analysis and identification of catabolic pathways for aromatic compounds in *Corynebacterium glutamicum*. *Microbes Environ.* **20**, 160–167
 32. Ault, A. (2004) The monosodium glutamate story: the commercial production of MSG and other amino acids. *J. Chem. Educ.* **81**, 347–355
 33. Becker, J., Zelder, O., Häfner, S., Schröder, H., and Wittmann, C. (2011) From zero to hero-Design-based systems metabolic engineering of *Corynebacterium glutamicum* for L-lysine production. *Metab. Eng.* **13**, 159–168
 34. Ikeda, M., Ohnishi, J., Hayashi, M., and Mitsuhashi, S. (2006) A genome-based approach to create a minimally mutated, *Corynebacterium glutamicum* strain for efficient L-lysine production. *J. Ind. Microbiol. Biotechnol.* **33**, 610–615
 35. Jojima, T., Fujii, M., Mori, E., Inui, M., and Yukawa, H. (2010) Engineering of sugar metabolism of *Corynebacterium glutamicum* for production of amino acid L-alanine under oxygen deprivation. *Appl. Microbiol. Biotechnol.* **87**, 159–165
 36. Peters-Wendisch, P., Stolz, M., Etterich, H., Kennerknecht, N., Sahn, H., and Eggeling, L. (2005) Metabolic engineering of *Corynebacterium glutamicum* for L-serine production. *Appl. Environ. Microbiol.* **71**, 7139–7144
 37. Stäbler, N., Oikawa, T., Bott, M., and Eggeling, L. (2011) *Corynebacterium glutamicum* as a host for synthesis and export of D-amino acids. *J. Bacteriol.* **193**, 1702–1709
 38. Hannemann, F., Bichet, A., Ewen, K. M., and Bernhardt, R. (2007) Cytochrome P450 systems: biological variations of electron transport chains. *Biochim. Biophys. Acta* **1770**, 330–344
 39. Anzai, Y., Li, S., Chaulagain, M. R., Kinoshita, K., Kato, F., Montgomery, J., and Sherman, D. H. (2008) Functional analysis of MycCI and MycG, cytochrome P450 enzymes involved in biosynthesis of mycinamicin macrolide antibiotics. *Chem. Biol.* **15**, 950–959
 40. Kieser, T., Bibb, M. J., Buttner, M. J., Chater, K. F., and Hopwood, D. A. (2000) *Practical Streptomyces Genetics*, John Innes Foundation, Norwich, UK
 41. Green, M. R., and Sambrook, J. (2012) *Molecular Cloning: A Laboratory Manual*, 4th Ed., Cold Spring Harbor Laboratory, Cold Spring Harbor, New York
 42. Liu, Y., Wang, C., Yan, J. Y., Zhang, W., Guan, W. N., Lu, X. F., and Li, S. Y. (2014) Hydrogen peroxide-independent production of α -alkenes by OleT_{JE} P450 fatty acid decarboxylase. *Biotechnol. Biofuels* **7**, 28
 43. Omura, T., and Sato, R. (1964) The carbon monoxide-binding pigment of liver microsomes: II. solubilization, purification, and properties. *J. Biol. Chem.* **239**, 2379–2385
 44. Bradford, M. M. (1976) A rapid and sensitive method for the quantitation of microgram quantities of protein utilizing the principle of protein-dye binding. *Anal. Biochem.* **72**, 248–254
 45. Schmeling, S., Narmandakh, A., Schmitt, O., Gad'on, N., Schühle, K., and Fuchs, G. (2004) Phenylphosphate synthase: a new phosphotransferase catalyzing the first step in anaerobic phenol metabolism in *Thauera aromatica*. *J. Bacteriol.* **186**, 8044–8057
 46. McKenna, C. E., Higa, M. T., Cheung, N. H., and McKenna, M.-C. (1977) The facile dealkylation of phosphonic acid dialkyl esters by bromotrimethylsilane. *Tetrahedron Lett.* **18**, 155–158
 47. Kenner, G. W., and Williams, N. R. (1955) A method of reducing phenols to aromatic hydrocarbons. *J. Chem. Soc.* 522–525
 48. Werck-Reichhart, D., and Feyereisen, R. (2000) Cytochromes P450: a success story. *Genome Biol.* **1**, reviews3003
 49. Keat, M. J., and Hopper, D. J. (1978) *para*-Cresol and 3,5-xyleneol methylhydroxylases in *Pseudomonas putida* Ncib-9869. *Biochem. J.* **175**, 649–658
 50. Johannes, J., Bluschke, A., Jehmlich, N., von Bergen, M., and Boll, M. (2008) Purification and characterization of active-site components of the putative *p*-cresol methylhydroxylase membrane complex from *Geobacter metallireducens*. *J. Bacteriol.* **190**, 6493–6500
 51. Herzberg, O., Chen, C. C., Kapadia, G., McGuire, M., Carroll, L. J., Noh, S. J., and Dunaway-Mariano, D. (1996) Swiveling-domain mechanism for enzymatic phosphotransfer between remote reaction sites. *Proc. Natl. Acad. Sci. U.S.A.* **93**, 2652–2657
 52. Hanukoglu, I. (1996) Electron transfer proteins of cytochrome P450 systems. in *Advances in Molecular and Cell Biology*, JAI Press Inc., Stamford, CT
 53. Ding, W., Si, M. R., Zhang, W. P., Zhang, Y. L., Chen, C., Zhang, L., Lu, Z. Q., Chen, S. L., and Shen, X. H. (2015) Functional characterization of a vanillin dehydrogenase in *Corynebacterium glutamicum*. *Sci. Rep.* **5**, 8044
 54. Chen, Y. F., Chao, H., and Zhou, N. Y. (2014) The catabolism of 2,4-xyleneol and *p*-cresol share the enzymes for the oxidation of *para*-methyl group in *Pseudomonas putida* NCIMB 9866. *Appl. Microbiol. Biotechnol.* **98**, 1349–1356
 55. Di Gioia, D., Luziatelli, F., Negroni, A., Ficca, A. G., Fava, F., and Ruzzi, M. (2010) Metabolic engineering of *Pseudomonas fluorescens* for the production of vanillin from ferulic acid. *J. Biotechnol.* **156**, 309–316
 56. Breinig, S., Schiltz, E., and Fuchs, G. (2000) Genes involved in anaerobic metabolism of phenol in the bacterium *Thauera aromatica*. *J. Bacteriol.* **182**, 5849–5863
 57. Schühle, K., and Fuchs, G. (2004) Phenylphosphate carboxylase: a new C-C lyase involved in anaerobic in phenol metabolism in *Thauera aromatica*. *J. Bacteriol.* **186**, 4556–4567
 58. Li, S., Chaulagain, M. R., Knauff, A. R., Podust, L. M., Montgomery, J., and Sherman, D. H. (2009) Selective oxidation of carbolide C-H bonds by an engineered macrolide P450 mono-oxygenase. *Proc. Natl. Acad. Sci. U.S.A.* **106**, 18463–18468
 59. Sherman, D. H., Li, S., Yermalitskaya, L. V., Kim, Y., Smith, J. A., Waterman, M. R., and Podust, L. M. (2006) The structural basis for substrate anchoring, active site selectivity, and product formation by P450 PikC from *Streptomyces venezuelae*. *J. Biol. Chem.* **281**, 26289–26297
 60. Tudzynski, B., Hedden, P., Carrera, E., and Gaskin, P. (2001) The P450–4 gene of *Gibberella fujikuroi* encodes ent-kaurene oxidase in the gibberellin biosynthesis pathway. *Appl. Environ. Microbiol.* **67**, 3514–3522
 61. Ro, D. K., Paradise, E. M., Ouellet, M., Fisher, K. J., Newman, K. L., Ndungu, J. M., Ho, K. A., Eachus, R. A., Ham, T. S., Kirby, J., Chang, M. C.,

4-Cresol Catabolic Pathway Initiated by Phosphorylation

- Withers, S. T., Shiba, Y., Sarpong, R., and Keasling, J. D. (2006) Production of the antimalarial drug precursor artemisinic acid in engineered yeast. *Nature* **440**, 940–943
62. Paddon, C. J., Westfall, P. J., Pitera, D. J., Benjamin, K., Fisher, K., McPhee, D., Leavell, M. D., Tai, A., Main, A., Eng, D., Polichuk, D. R., Teoh, K. H., Reed, D. W., Treynor, T., Lenihan, J., *et al.* (2013) High-level semi-synthetic production of the potent antimalarial artemisinin. *Nature* **496**, 528–532
63. Carlson, J. C., Li, S., Gunatilleke, S. S., Anzai, Y., Burr, D. A., Podust, L. M., and Sherman, D. H. (2011) Tirandamycin biosynthesis is mediated by co-dependent oxidative enzymes. *Nat. Chem.* **3**, 628–633
64. Bernhardt, R., and Urlacher, V. B. (2014) Cytochromes P450 as promising catalysts for biotechnological application: chances and limitations. *Appl. Microbiol. Biotechnol.* **98**, 6185–6203

Supporting Information

Characterization of a Unique Pathway for 4-Cresol Catabolism Initiated by Phosphorylation in *Corynebacterium glutamicum*

Lei Du^{1,2}, Li Ma¹, Feifei Qi¹, Xianliang Zheng^{1,2}, Chengying Jiang³, Ailei Li⁴, Xiaobo Wan⁴, Shuang-Jiang Liu^{3*}, Shengying Li^{1*}

¹CAS Key Laboratory of Biofuels, Shandong Provincial Key Laboratory of Synthetic Biology, and

⁴CAS Key Laboratory of Bio-based Materials at Qingdao Institute of Bioenergy and Bioprocess Technology, Chinese Academy of Sciences, Qingdao, Shandong 266101, China

²University of Chinese Academy of Sciences, Beijing 100049, China

³State Key Laboratory of Microbial Resources, and Environmental Microbiology and Biotechnology Research Center at Institute of Microbiology, Chinese Academy of Sciences, Beijing 100101, China

Running title: *The 4-Cresol Catabolic Pathway Initiated by Phosphorylation*

*To whom correspondence may be addressed. E-mail: lishengying@qibebt.ac.cn (Li S.), liusj@im.ac.cn (Liu S.-J.)

Keywords: 4-cresol, biodegradation, *Corynebacterium glutamicum*, cytochrome P450 monooxygenase, phosphorylation

Table of Contents

Supporting Information Text.....	S-3
Table S1	S-4
Table S2	S-5
Figure S1.....	S-6
Figure S2.....	S-6
Figure S3.....	S-7
Figure S4.....	S-7
Figure S5.....	S-8
Figure S6.....	S-8
Figure S7.....	S-9
Figure S8.....	S-9
Figure S9.....	S-10
Figure S10.....	S-10
Figure S11	S-11
Figure S12.....	S-11
Figure S13.....	S-12
Figure S14.....	S-12
Figure S15.....	S-12
Figure S16.....	S-13
Figure S17.....	S-13
Figure S18.....	S-13
Figure S19.....	S-14
Figure S20.....	S-14
Figure S21.....	S-14
Figure S22.....	S-15
Figure S23.....	S-15
Figure S24.....	S-15
Figure S25.....	S-16

Supporting Information Text

Synthesis of diethyl (4-formylphenyl) phosphate. To a solution of 4-hydroxybenzyl aldehyde (2.3 g, 19 mmol) dissolved in carbon tetrachloride (20 mL) was added diethyl phosphite (2.9 mL, 23 mmol) at 0 °C under argon atmosphere. Triethylamine (3.2 mL, 23 mmol) was carefully added drop-wise to the mixture by using a dropping funnel. The mixture was stirred overnight at room temperature. Water (50 mL) was added and the organic layer was separated. The organic layer was washed twice with dilute hydrochloric acid (2 × 25 mL), four times with dilute sodium hydroxide solution (4 × 25 mL), and twice with brine (2 × 25 mL) before being dried over anhydrous MgSO₄. Removal of solvent on rotary evaporator gave a crude, which was further purified by silica gel column chromatography using a petroleum ether/ethyl acetate (4/1: v/v) mixture to afford diethyl (4-formylphenyl) phosphate (3.5 g). Yield: 71%.

Synthesis of diethyl (4-(hydroxymethyl)phenyl) phosphate. To a solution of diethyl (4-formylphenyl) phosphate (1.5 g, 5.8 mmol) dissolved in absolute ethyl alcohol (20 mL) at 0 °C was added sodium borohydride (0.29 g, 7.5 mmol) portion wise. The reaction mixture was then warmed to room temperature and stirred for 30 min. The reaction was quenched with water (10 mL). Ethanol was evaporated and the resulting mixture was extracted with CH₂Cl₂ (2 × 30 mL). The extract was washed with brine (30 mL), and dried over anhydrous MgSO₄. Removal of solvent on rotary evaporator gave a crude, which was further purified by silica gel column chromatography using a petroleum ether/ethyl acetate (1/2: v/v) mixture to afford diethyl (4-(hydroxymethyl)phenyl) phosphate (1.4 g). Yield: 95%.

Synthesis of compound benzylalcohol-4-phosphate. Diethyl (4-(hydroxymethyl)phenyl) phosphate (0.74 g, 2.9 mmol) was dissolved in dry CH₂Cl₂ (25 mL). Then bromotrimethylsilane (3.8 mL, 10 equiv. to phosphate ester) was added to the solution and the mixture was heated to reflux for 18 h under argon atmosphere. The solvent was evaporated and the residue was dissolved in anhydrous methanol (25 mL). The solution was stirred for 30 min at 40 °C. Then the resulting solution was concentrated to give benzylalcohol-4-phosphate (0.53 g). Yield: 90%.

Synthesis of compound benzylaldehyde-4-phosphate. The detailed procedures were the same as synthesis of benzylalcohol-4-phosphate with using diethyl (4-formylphenyl) phosphate as the reaction substrate. Yield: 91%.

Synthesis of diethyl 4-tolyl phosphate. The detailed procedures were the same as synthesis of diethyl (4-formylphenyl) phosphate with using 4-cresol as the reaction substrate. Yield: 80%.

Synthesis of compound 4-methylbenzyl phosphate. The detailed procedures were the same as synthesis of benzylalcohol-4-phosphate with using diethyl 4-tolyl phosphate as the reaction substrate. Yield: 92%.

Table S1: Strains and plasmids used in this study

Strain, plasmid	genotype/phenotype	Source
<i>E. coli</i> BL21(DE3)		Novagen
<i>E. coli</i> DH5 α		Invitrogen
<i>C. glutamicum</i> RES167	restriction-deficient mutant of ATCC13032, $\Delta(cglIM-cglIR-cglIIR)$	Li T, <i>et al.</i> , 2014
pET28b	expression vector	Novagen
pET28b- <i>creC</i>	pET28b derivative for expression of <i>creC</i>	Present study
pET28a- <i>creD</i>	pET28a derivative for expression of <i>creD</i>	Li T, <i>et al.</i> , 2014
pET28a- <i>creE</i>	pET28a derivative for expression of <i>creE</i>	Li T, <i>et al.</i> , 2014
pET28a- <i>creF</i>	pET28a derivative for expression of <i>creF</i>	Li T, <i>et al.</i> , 2014
pET28a- <i>creG</i>	pET28a derivative for expression of <i>creG</i>	Li T, <i>et al.</i> , 2014
pET28b- <i>creH</i>	pET28b derivative for expression of <i>creH</i>	Present study
pET28b- <i>creI</i>	pET28b derivative for expression of <i>creI</i>	Present study
pET28a- <i>creJ</i>	pET28a derivative for expression of <i>creJ</i>	Li T, <i>et al.</i> , 2014

Table S2: Primers used in this study

Primers	Sequences (5'-3')	Description
creC-F	CCGCCATATGCCGATGAATGCTGCAACCA	To construct pET28b- <i>creC</i>
creC-R	GCGCGGATCCGTGTTTAGCTGAGAACTTTCAG	To construct pET28b- <i>creC</i>
creD-F	GACACATATGACTCGCAGTAATTTACCCGC	To construct pET28b- <i>creD</i>
creD-R	CGGAATTCGAGAAGCACGCCTGGTTG	To construct pET28b- <i>creD</i>
creE-F	GACACATATGAATACTTCAGCTGAAACTGGA	To construct pET28b- <i>creE</i>
creE-R	GGAGCTCTCCCAAGCGGGTAAAT	To construct pET28b- <i>creE</i>
creF-F	GCGCCATATG AAGATCATGTCTACTATTCATT	To construct pET28b- <i>creF</i>
creF-R	TCATAAGCTT TCACACTTGCCTTCTGGCG	To construct pET28b- <i>creF</i>
creG-F	GACACATATGCCTAGTCCACGCACTGTTC	To construct pET28b- <i>creG</i>
creG-R	CGGAATTCAGTAGACATGATCTTCTCCTTAG	To construct pET28b- <i>creG</i>
creH-F	GCGCCATATGGCTAATAAATCTTTCCCAAGCCC	To construct pET28b- <i>creH</i>
creH-R	ACGCGGATCCGTGGACTAGGCATGTGTATC	To construct pET28b- <i>creH</i>
creI-F	TCGCCATATGGGAGACACCATGACCAACAGT	To construct pET28b- <i>creI</i>
creI-R	GCCCAAGCTTAACGAGGTAGTACGGGTACA	To construct pET28b- <i>creI</i>
creJ-R	CGTGCCATGGGCACAATGACTTCCAGACT	To construct pET28b- <i>creJ</i>
creJ-R	CGGGAAGCTTAGCGTTCCAAGTCACGGGAA	To construct pET28b- <i>creJ</i>
CB-F	TCTCGGTGGCTTGGTATT	RT-PCR. To amplify region a in Figure S11.
CB-R	AAGATTCGGCGATGACTG	RT-PCR. To amplify region a in Figure S11.
DC-F	GGCTTCTAGCTCATGGTTCG	RT-PCR. To amplify region b in Figure S11.
DC-R	AATGGGCGGATGTCTTCG	RT-PCR. To amplify region b in Figure S11.
DE-F	CTCAAACACTACAAATTGCAGGAC	RT-PCR. To amplify region c in Figure S11.
DE-R	CGGAGATGATTCCGGCTCT	RT-PCR. To amplify region c in Figure S11.
FE-F	GGCGGTTCCCTTATCGTGT	RT-PCR. To amplify region d in Figure S11.
FE-R	GATCCGTCGTCGTTCTTTT	RT-PCR. To amplify region d in Figure S11.
GF-F	ACCAGGGTGCTTGCTAAA	RT-PCR. To amplify region e in Figure S11.
GF-R	GGACTGCGGTCTCCATTA	RT-PCR. To amplify region e in Figure S11.
HG-F	AAAACCGGCGATTACCTC	RT-PCR. To amplify region f in Figure S11.
HG-R	GCTCTTTAGCAAGCACCT	RT-PCR. To amplify region f in Figure S11.
IH-F	AAGCCCCTTGATGAAGAA	RT-PCR. To amplify region g in Figure S11.
IH-R	TGAATCGCAGAACCAGAAT	RT-PCR. To amplify region g in Figure S11.
JI-F	TGGTTTCGGCATCCACTA	RT-PCR. To amplify region h in Figure S11.
JI-R	GAAGCCCAGCATTTACGG	RT-PCR. To amplify region h in Figure S11.
RJ-F	CGCTATCTCCCGATCCTT	RT-PCR. To amplify region i in Figure S11.
RJ-R	AACATCACTGGCTCTTCCT	RT-PCR. To amplify region i in Figure S11.
R-F	CGATGCGGTATAGAACGA	RT-PCR. To amplify region j in Figure S11.
R-R	GAAACGAGACGGTGGGTG	RT-PCR. To amplify region j in Figure S11.

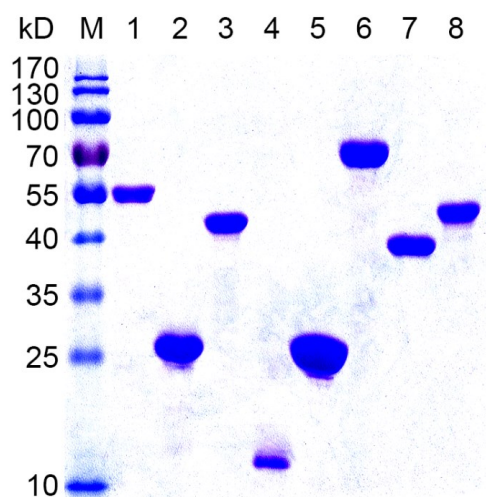


Figure S1. SDS-PAGE analysis of purified proteins. M, marker; 1, CreC; 2, CreD; 3, CreE; 4, CreF; 5, CreG; 6, CreH; 7, CreI; 8, CreJ.

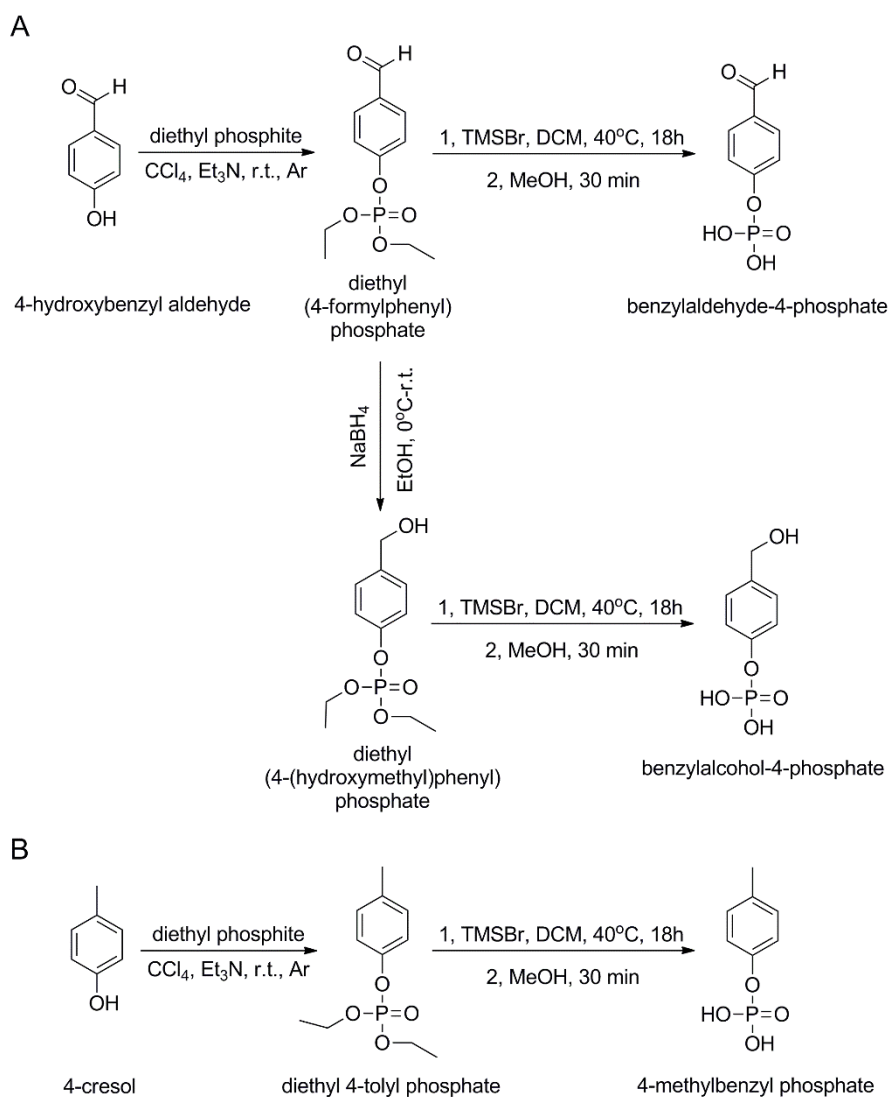


Figure S2. Chemical synthesis routes of 4-methylbenzyl phosphate, benzylalcohol-4-phosphate and benzylaldehyde-4-phosphate.

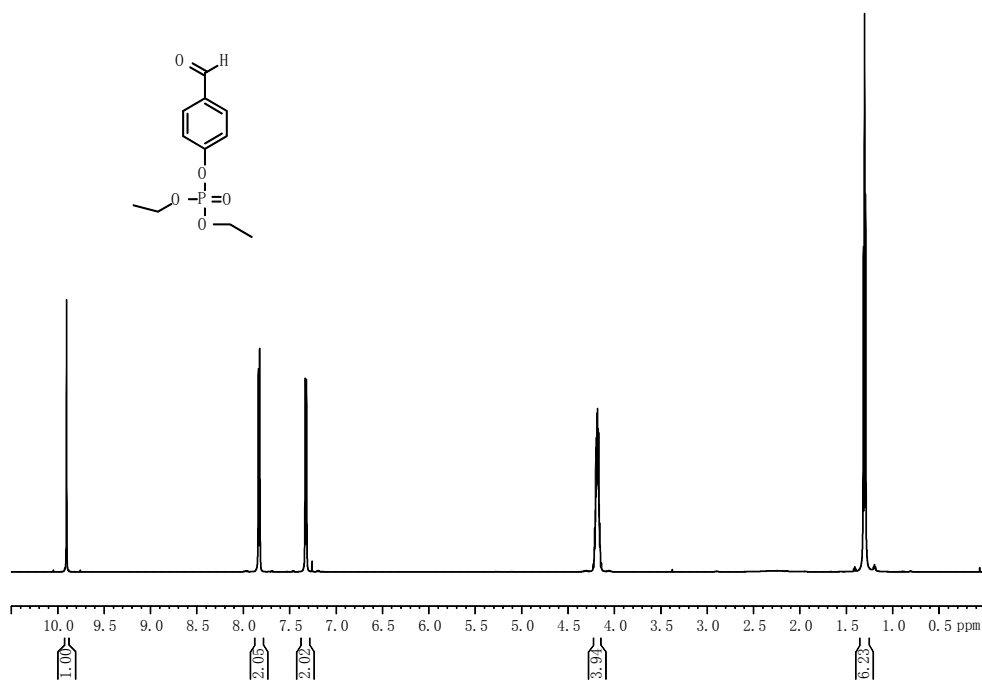


Figure S3. ¹H NMR spectrum of diethyl (4-formylphenyl) phosphate in CDCl₃.

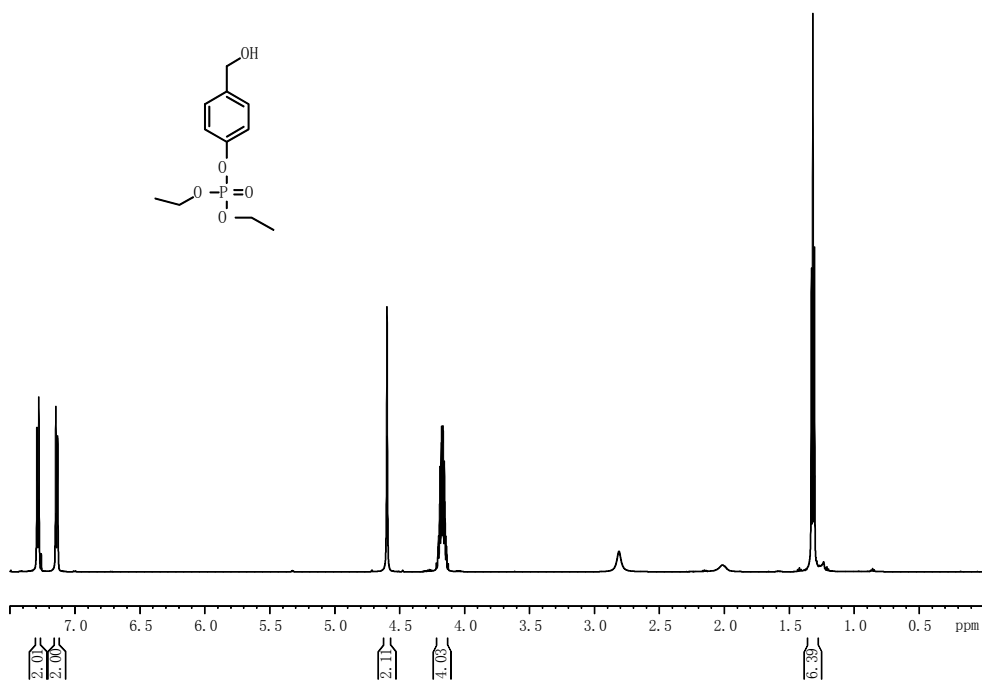


Figure S4. ¹H NMR spectrum of diethyl (4-(hydroxymethyl)phenyl) phosphate in CDCl₃.

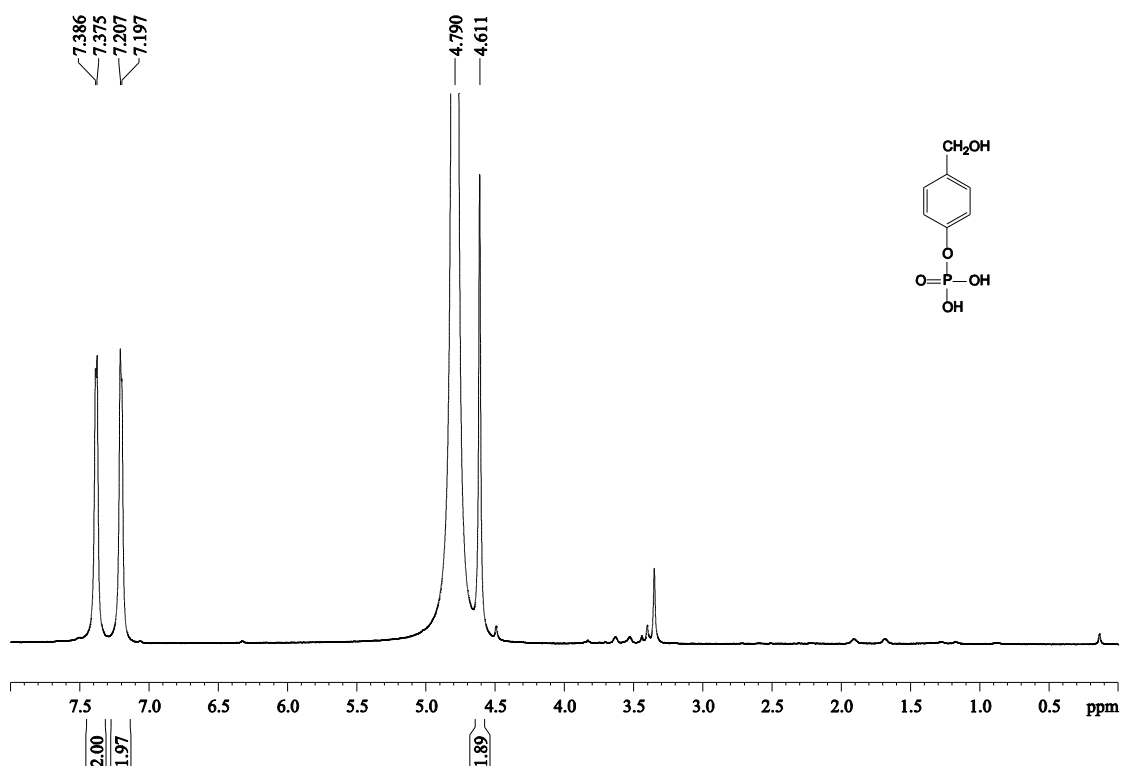


Figure S5. ^1H NMR spectrum of benzylalcohol-4-phosphate in D_2O .

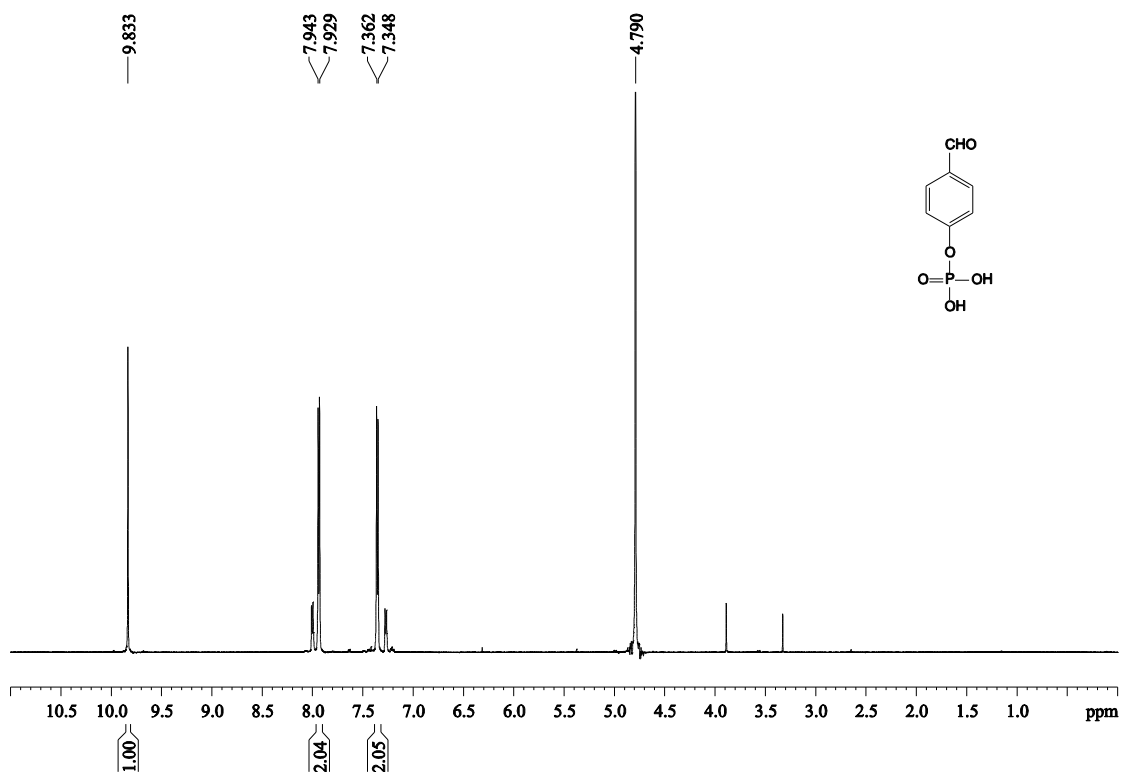


Figure S6. ^1H NMR spectrum of benzylaldehyde-4-phosphate in D_2O .

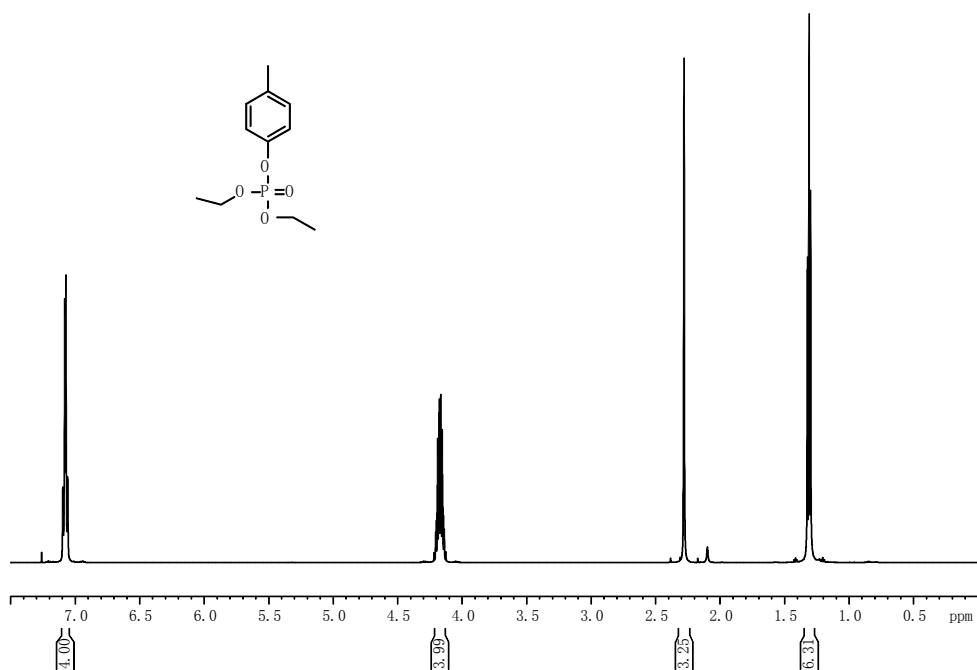


Figure S7. ^1H NMR spectrum of diethyl 4-tolyl phosphate in CDCl_3 .

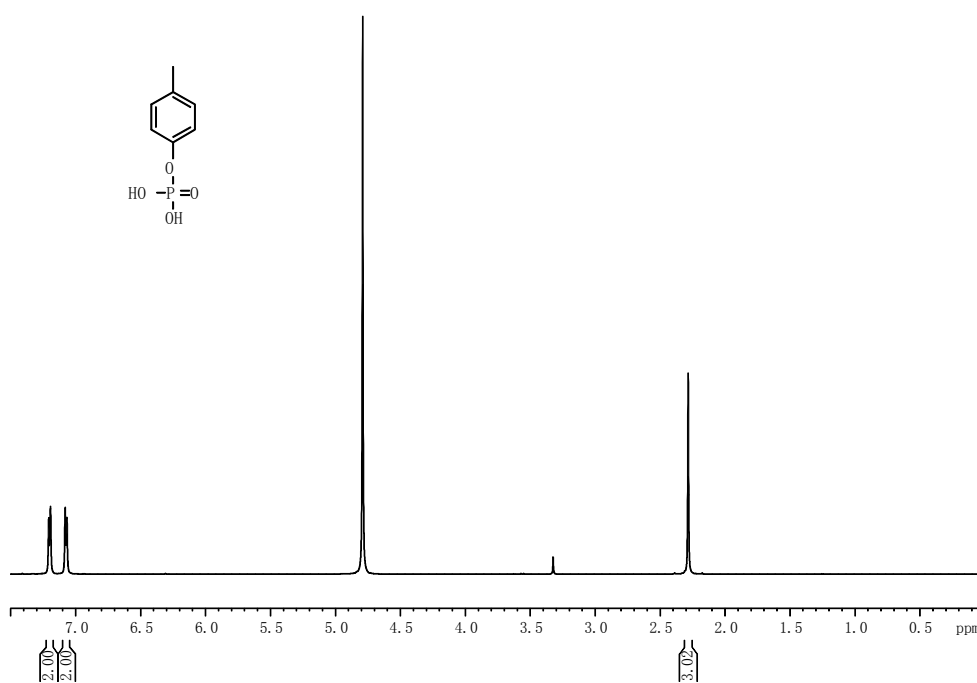


Figure S8. ^1H NMR spectrum of 4-methylbenzyl phosphate in D_2O .

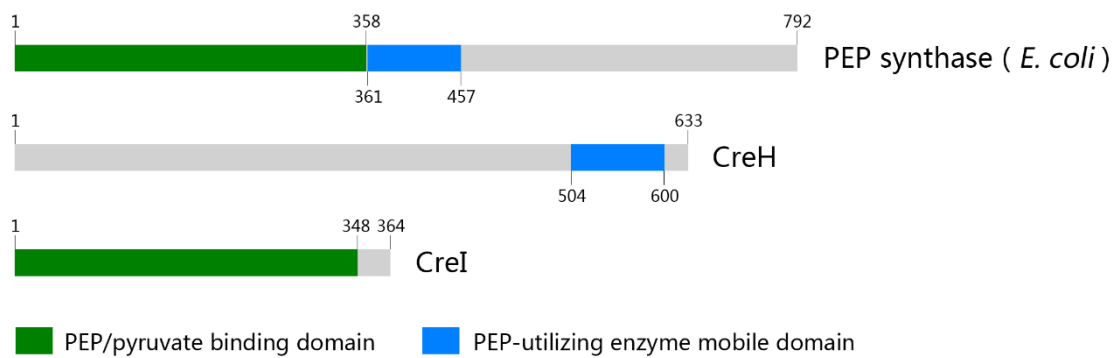


Figure S9. Conserved domain analysis of the PEP synthase of *E. coli*, CreH and CreI.

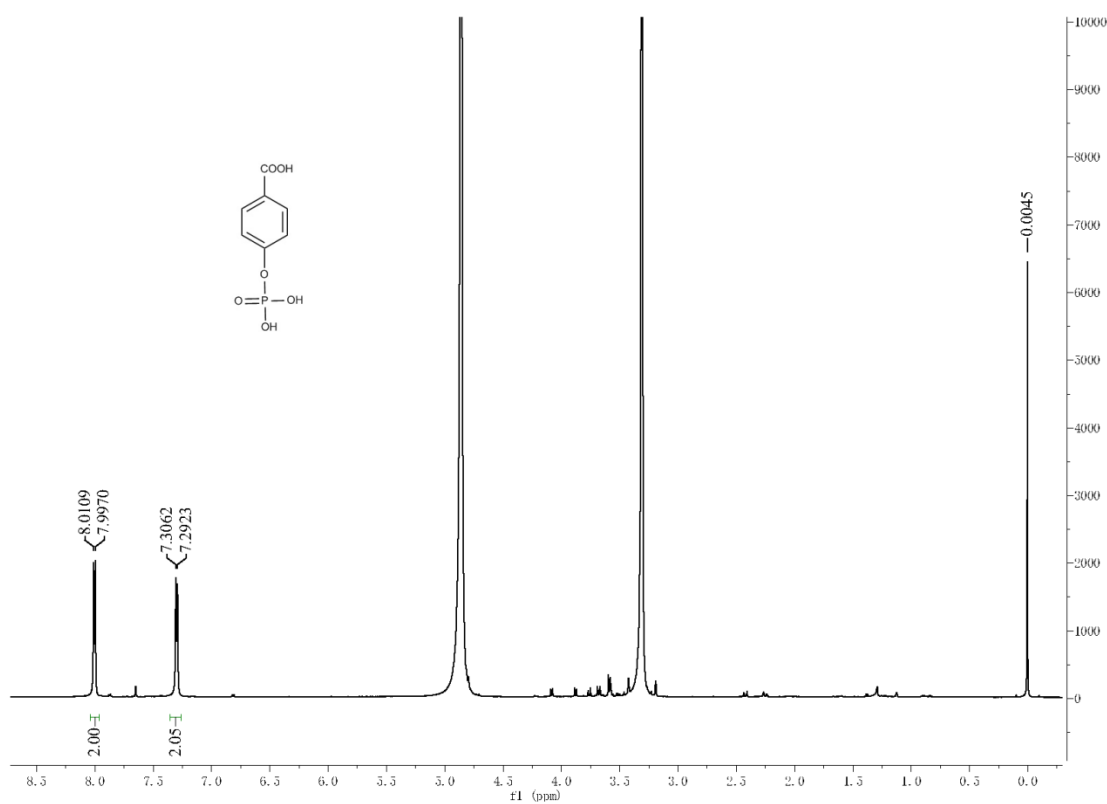


Figure S10. ^1H NMR spectrum of benzoate-4-phosphate in D_2O .

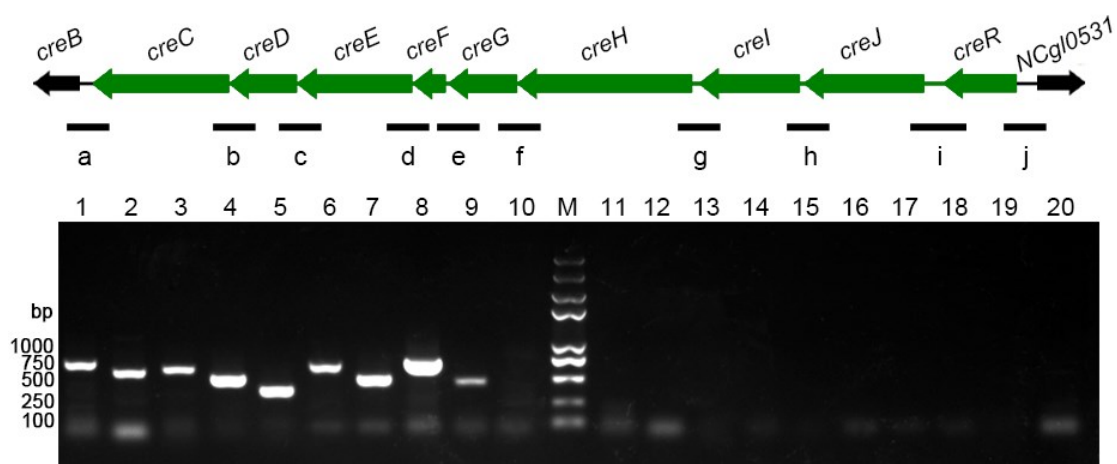


Figure S11. Results of RT-PCR assays. The cDNA prepared from *Corynebacterium glutamicum* RES167 grown in LB broth containing 2 mM 4-cresol for 48 h was used as template. Black bars below the gene cluster (a to j) represent the locations of fragments amplified from RT-PCR assays. Lanes 1-10 show the a-j RT-PCR products. Lanes 11-20 were negative controls with mRNA as PCR template. M: Molecular size standard.

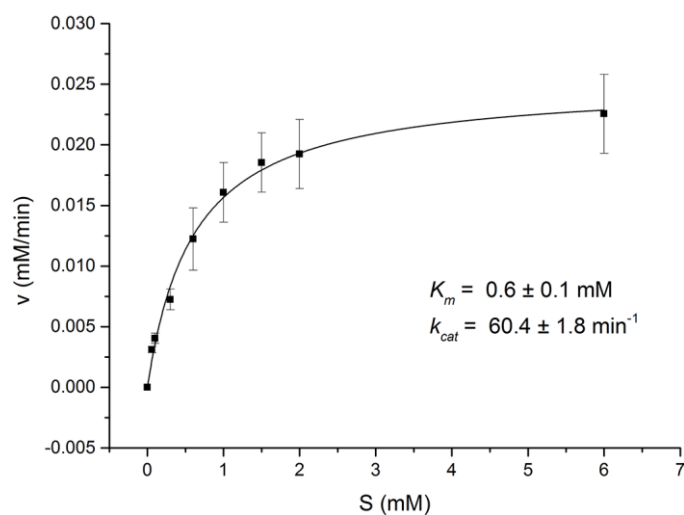


Figure S12. The kinetic curve of CreHI with 4-cresol as substrate. ($[\text{CreH}] = [\text{CreI}] = 1.7 \mu\text{M}$)

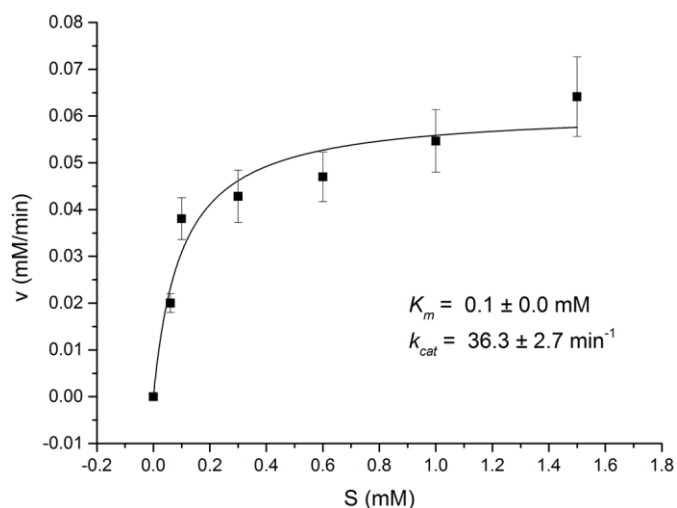


Figure S13. The kinetic curve of CreHI with 4-hydroxybenzyl alcohol as substrate. ([CreH] = [CreI] = 1.7 μ M)

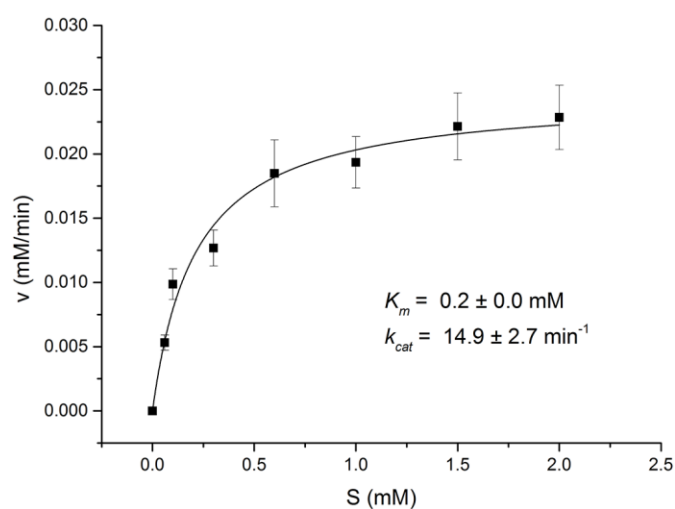


Figure S14. The kinetic curve of CreHI with 4-hydroxybenzyl aldehyde as substrate. ([CreH] = [CreI] = 1.7 μ M)

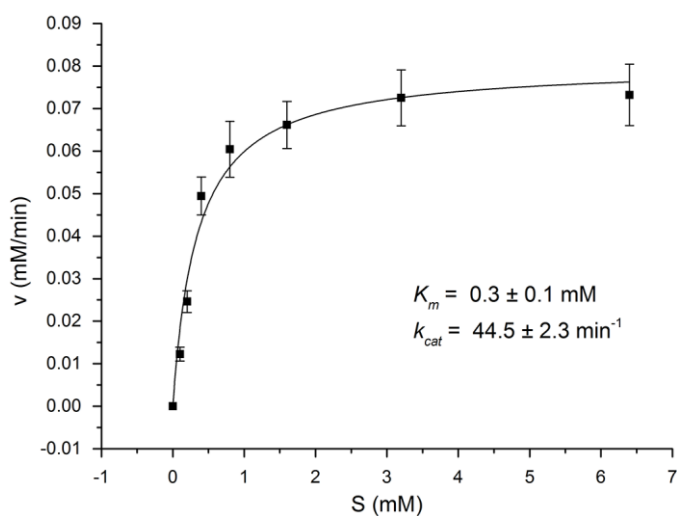


Figure S15. The kinetic curve of CreJEF with 4-methylbenzyl phosphate as substrate. ([CreJ] = [CreE] = [CreF] = 0.8 μ M)

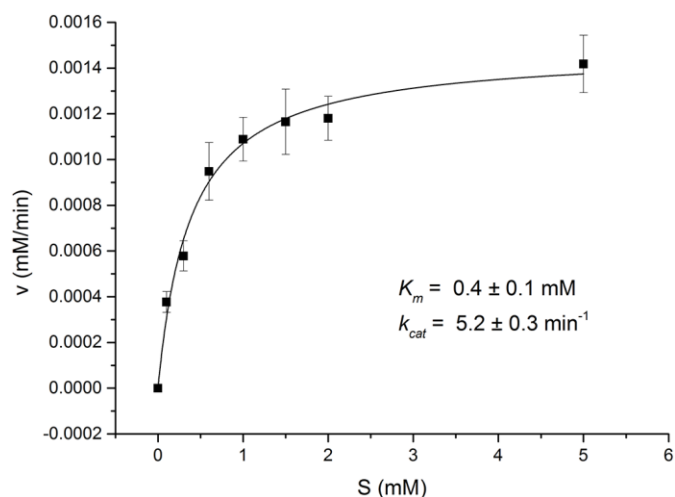


Figure S16. The kinetic curve of CreJEF with benzylalcohol-4-phosphate as substrate. ($[\text{CreJ}] = [\text{CreE}] = [\text{CreF}] = 0.8 \mu\text{M}$)

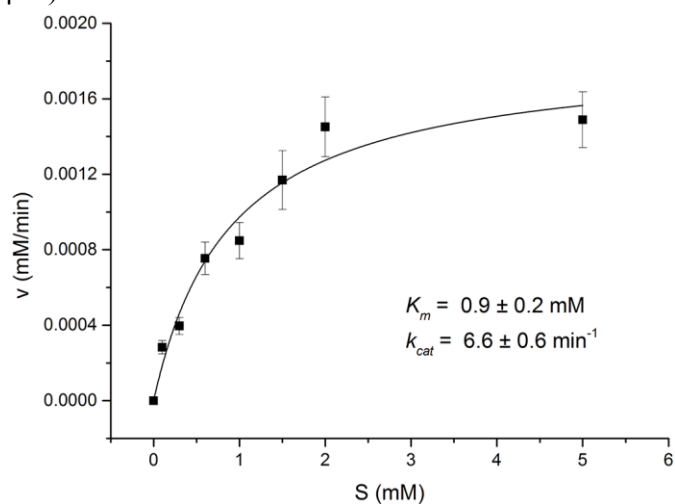


Figure S17. The kinetic curve of CreJEF with benzylaldehyde-4-phosphate as substrate. ($[\text{CreJ}] = [\text{CreE}] = [\text{CreF}] = 0.8 \mu\text{M}$)

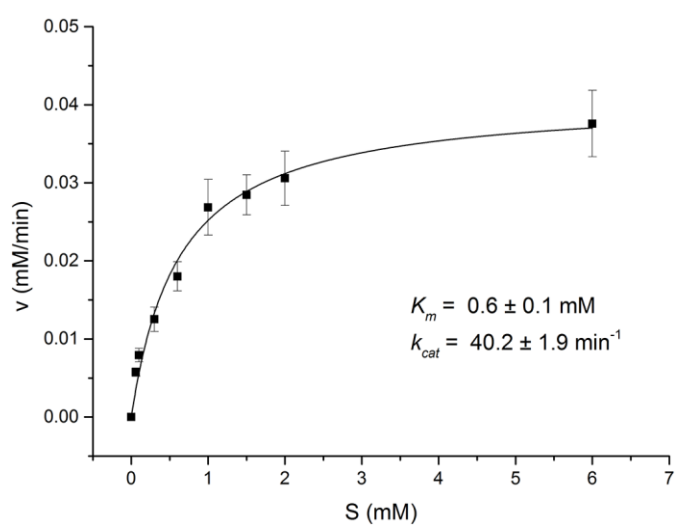


Figure S18. The kinetic curve of CreD with 4-methylbenzyl phosphate as substrate. ($[\text{CreD}] = 1.0 \mu\text{M}$)

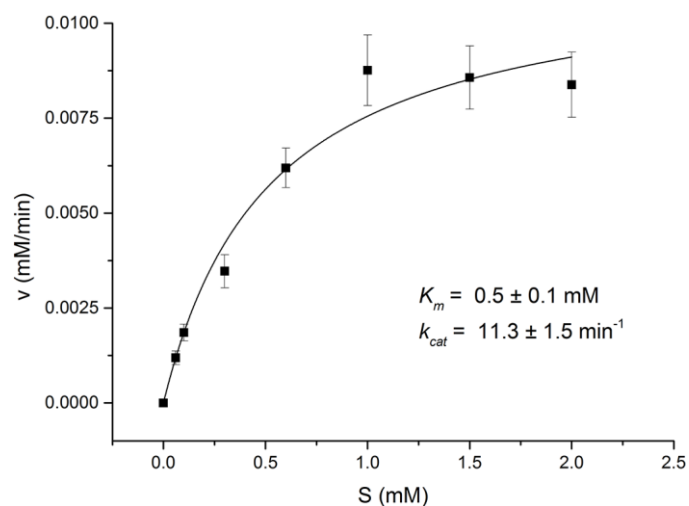


Figure S19. The kinetic curve of CreD with benzylalcohol-4-phosphate as substrate. ([CreD] = 1.0 μM)

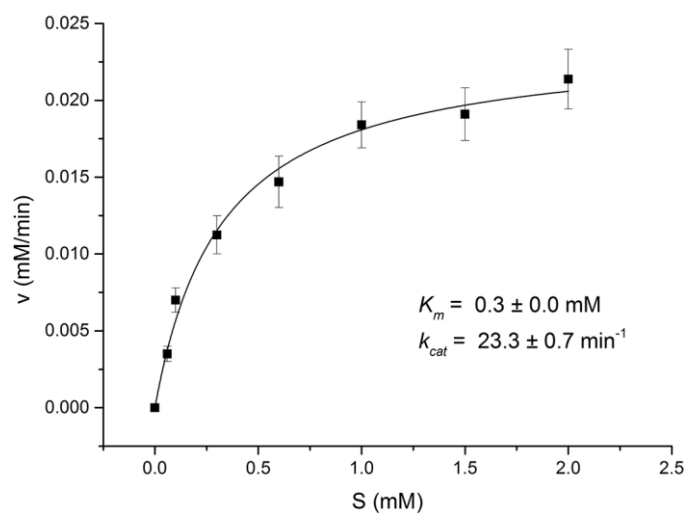


Figure S20. The kinetic curve of CreD with benzylaldehyde-4-phosphate as substrate. ([CreD] = 1.0 μM)

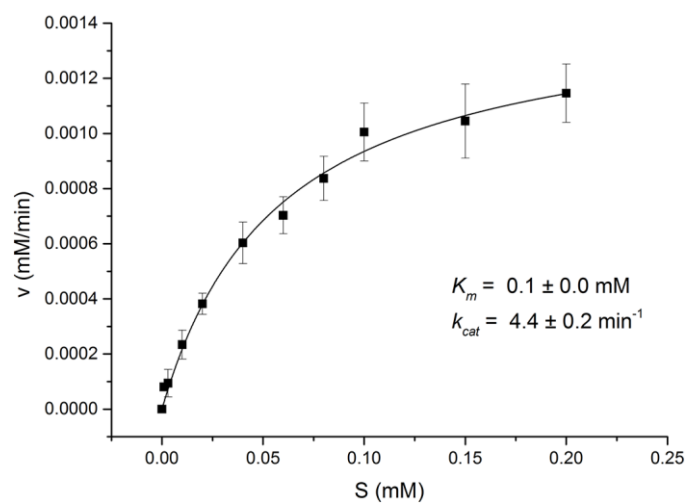


Figure S21. The kinetic curve of CreC with 4-hydroxybenzyl aldehyde as substrate. ([CreC] = 0.3 μM)

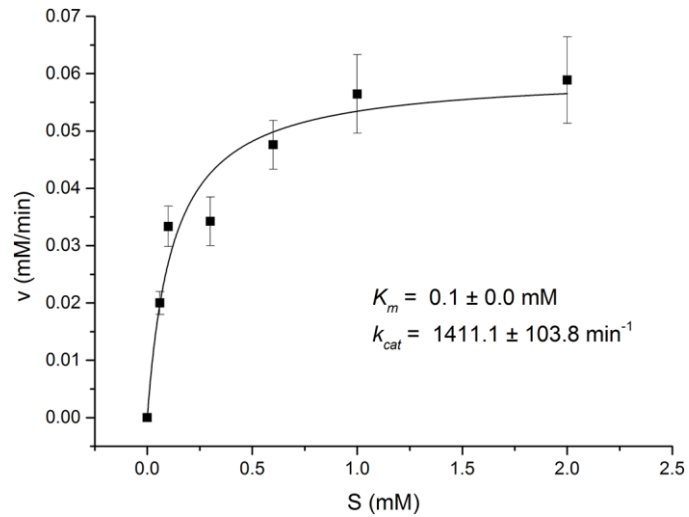


Figure S22. The kinetic curve of CreC with benzylaldehyde-4-phosphate as substrate. ($[\text{CreC}] = 0.04 \mu\text{M}$)

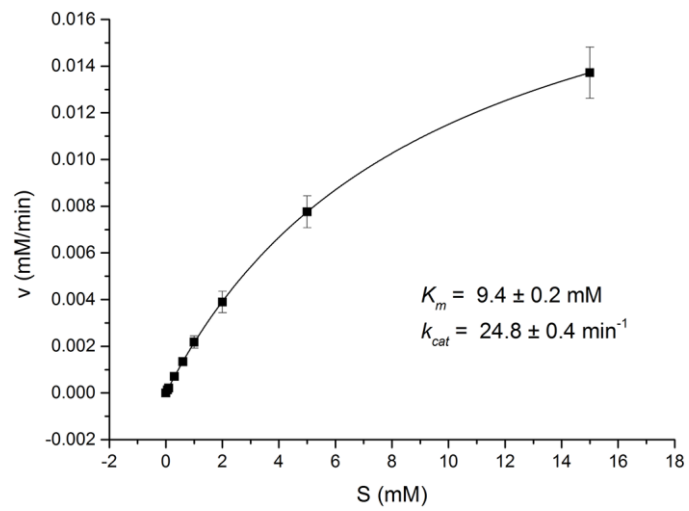


Figure S23. The kinetic curve of CreG with 4-hydroxybenzyl alcohol as substrate. ($[\text{CreG}] = 0.9 \mu\text{M}$)

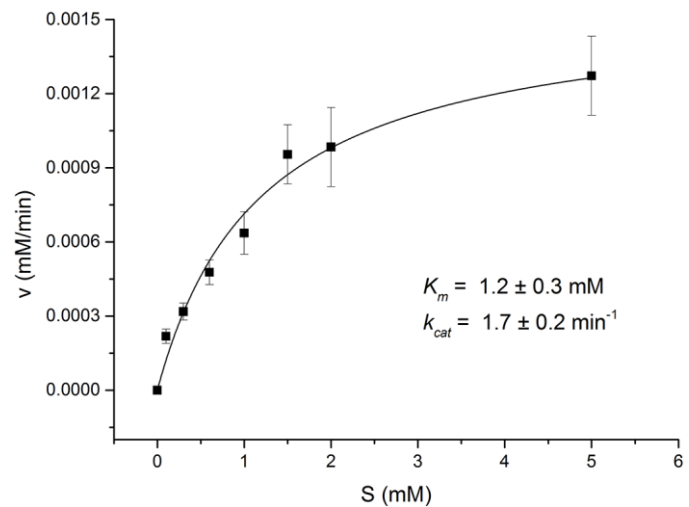


Figure S24. The kinetic curve of CreG with benzylalcohol-4-phosphate as substrate. ($[\text{CreG}] = 0.9 \mu\text{M}$)

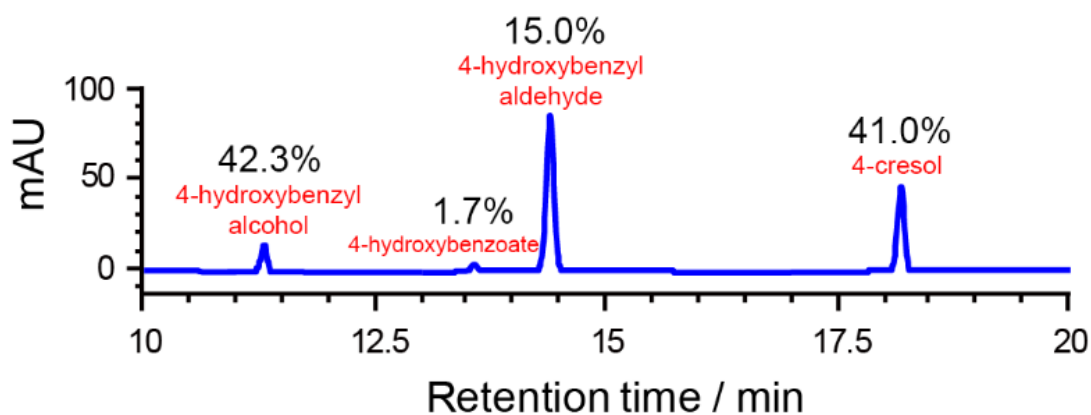


Figure S25. HPLC analysis of the competition assay between CreJEF and CreD. In this assay, 1 mM 4-methylbenzyl phosphate was used as substrate, and all involved enzymes were normalized to the same concentration of 12.0 μ M. Assays were carried out in 100 mM Tris-HCl buffer (pH 8.0) at 30°C for 120 min. Each compound was quantified based on area under curve of corresponding HPLC peak relative to that of authentic standard compound with known concentration. Due to distinct extinction coefficients, the peak intensity of compounds do not necessarily reflect relative amounts shown in percentage.

Characterization of a Unique Pathway for 4-Cresol Catabolism Initiated by Phosphorylation in *Corynebacterium glutamicum*
Lei Du, Li Ma, Feifei Qi, Xianliang Zheng, Chengying Jiang, Ailei Li, Xiaobo Wan, Shuang-Jiang Liu and Shengying Li

J. Biol. Chem. 2016, 291:6583-6594.

doi: 10.1074/jbc.M115.695320 originally published online January 27, 2016

Access the most updated version of this article at doi: [10.1074/jbc.M115.695320](https://doi.org/10.1074/jbc.M115.695320)

Alerts:

- [When this article is cited](#)
- [When a correction for this article is posted](#)

[Click here](#) to choose from all of JBC's e-mail alerts

Supplemental material:

<http://www.jbc.org/content/suppl/2016/01/27/M115.695320.DC1.html>

This article cites 57 references, 23 of which can be accessed free at <http://www.jbc.org/content/291/12/6583.full.html#ref-list-1>